Copyright Warning & Restrictions

The copyright law of the United States (Title 17, United States Code) governs the making of photocopies or other reproductions of copyrighted material.

Under certain conditions specified in the law, libraries and archives are authorized to furnish a photocopy or other reproduction. One of these specified conditions is that the photocopy or reproduction is not to be "used for any purpose other than private study, scholarship, or research." If a, user makes a request for, or later uses, a photocopy or reproduction for purposes in excess of "fair use" that user may be liable for copyright infringement,

This institution reserves the right to refuse to accept a copying order if, in its judgment, fulfillment of the order would involve violation of copyright law.

Please Note: The author retains the copyright while the New Jersey Institute of Technology reserves the right to distribute this thesis or dissertation

Printing note: If you do not wish to print this page, then select "Pages from: first page # to: last page #" on the print dialog screen

NJIT
New Jersey's Science &
Technology University

The Van Houten library has removed some of the personal information and all signatures from the approval page and biographical sketches of theses and dissertations in order to protect the identity of NJIT graduates and faculty.

CHARACTERIZATION OF LPCVD DEPOSITED SILICON DIOXIDE THIN FILMS

By

Xue Du

A thesis submitted to the faculty of the graduate school of
New Jersey Institute of Technology for the
degree of Master of Science in Chemistry

Jan.03, 1992

Approval Sheet

Title of thesis: Characterization of LPCVD deposited silicon dioxide thin films

Name of Candidate: Xue Du

Thesis and Abstract Approved:

-- ----------------------

Dr. J. M. Grow Date

Department of Chemical Engineering,

Chemistry & Environmental Science

-- ----------------------

Dr. R. A. Levy Date

Department of Physics

-- ----------------------

Dr. T. Gund Date

Department of Chemical Engineering,

Chemistry & Environmental Science

ACKNOWLEDGEMENTS

I wish to express my sincere thanks to my advisor, Dr. J. M. Grow for his kind and abundant help, not only for this thesis but also for the whole time I spent for my master study in chemistry at New Jersey Institute of Technology in the past two years.

I also thank so much, Dr. R. A. Levy, my thesis advisor, the great help and financial support for my work and study.

A special thanks to Dr. T. Gund for her valuable suggestion to my paper work.

Also, my thanks to Mr. Chakrovarthy Srinivasa Gorthy, my partner, for his successful work done at deposition and valuable discussion. I wish to thank all my other colleagues in CVD lab at New Jersey Institute of Technology.

Finally, I wish to thank my husband and my little daughter, with their great help I can be myself today!

CHARACTERIZATION OF LPCVD DEPOSITED

SILICON DIOXIDE THIN FILMS

Abstract

LPCVD deposited amorphous silicon dioxide SiO_2 thin films from a new chemical vapor source, diethylsilane (DES), were characterized. This work is focused on evaluation of SiO_2 films prepared by varies deposition temperatures and flow rates series.

SiO_2 thin films were evaluated for density, porosity, and refractive index. Techniques for evaluation of the above mentioned parameters for this work included the use of infrared absorption spectroscopy, preferential etch procedures, optical measurement of refractive index and thickness, and thermal annealing of CVD films. The densification in vacuum ambient has been carried out at the temperature of 600 ^{o}, 750 ^{o}, and 900 ^{o}C, respectively.

The P-etch rates of SiO_2 thin films, produced using DES as a silicon source, were found to be in the range of 846 A/min. to 930 A/min. for a deposition temperatures between 375 ^{o} and 475 ^{o}C; while the etch rates were constant (about 900 A/min.) for SiO_2 films produced by varing diethylsilane flow rates between 20 and 150 sccm.

In the infrared absorption spectra, the strong Si-O-Si stretching band at the frequency 1070 cm $^{-1}$ shifted about 0 to 15 cm $^{-1}$ to high frequency, after annealing. The degree of shifting depends on the original deposition and the annealing temperature. Shiftings were also observed at the Si-O-Si bending and rocking bands at 800 and 450 cm $^{-1}$ respectively.

The ellipsometric measurement indicated the index of refraction for SiO_2 thin film to be 1.45 with no significant difference for samples with different deposition conditions.

CONTENTS

1. INTRODUCTION OF CVD FILM..........................1
1.1 A REVIEW OF CVD TECHNIQUES.................1
1.2 FUNDAMENTAL OF LPCVD REACTION..............3

2. LPCVD DEPOSITED SILICON DIOXIDE (SiO_2) FILM.......7
2.1 APPLICATION OF SiO_2 THIN FILM..............7
2.2 LOW-TEMPERATURE DEPOSITED SILICON DIOXIDE THIN FILM..........................9
2.3 NEW CHEMICAL SOURCE OF CVD DEPOSITED SiO_2 THIN FILMS............................9

3. CHARACTERIZATION OF SiO_2 FILM (Focus on DES flow rate and deposition temperature series)..............................11

3.1 INTRODUCTION..................................11
3.2 INFRARED SPECTROSCOPY...................... 16
3.2.1 Introduction of infrared spectroscopy..................................16
3.2.2 The application of infrared spectroscopy in SiO_2 thin film.............17

3.3 CHEMICAL ETCH TECHNIQUES...................22
3.3.1 Introduction of wet etching.........22
3.3.2 Basic etching theory................22
3.3.3 Chemical etching SiO_2...............23
3.3.4 P-etch for SiO_2 thin film...........24

3.4 THERMAL ANNEALING..........................25
3 4.1 Introduction of thermal annealing...25
3.4.2 The thermal annealing of SiO_2.......25

3.5 REFRACTIVE INDEX, ELLIPSOMETRY.............26
3.5.1 Introduction of ellipsometric technique..................................26
3.5.2 Basic physics of ellipsometry.......26
3.5.3 Refractive index measurement of silicon dioxide films...................30

3.6 THICKNESS MEASUREMENT......................30
3.6.1 The introduction of thin film thickness measurement method...............30
3.6.2 Silicon dioxide thin film thickness measurement......................31

4. EXPERIMENTAL RESULTS AND DISCUSSION...............34

4.1 INTRODUCTION..................................34

4.2 INFRARED SPECTROSCOPY.......................34
4.2.1 Effect of thickness on Si-O-Si absorption band..............................35
4.2.2 Effect of deposition temperature on absorption band.........................37
4.2.3 Effect of annealing temperature on SiO_2 thin film quality..................38
i. The annealing effect on the stretching and bending vibration of the SiO_2 thin film...............40
ii. The annealing effect on 3 um band of infrared spectra............45
iii. The annealing effect on the weak band at the frequency of 890 cm^{-1}.... 48
4.2.4 Effect of DES flow rate on Si-O-Si stretching band............................49
4.2.5 Effect of annealing temperature on Si-O-Si stretching band (DES flow rate series)..............................50

4.3 ETCHING RATE...............................51
4.3.1 Etching rate of silicon dioxide films with varies DES flow rate............51
4.3.2 Behavior of etching rate on deposition temperature series..............53
4.3.3 The different annealing temperature effect on the etching rate of silicon dioxide films..............57
4 3.4 Temperature effect on etching rate of silicon dioxide films..............59

4.4 REFRACTIVE INDEX MEASUREMENT...............62
4.4.1 Deposition temperature series.......62
4.4.2 Effect of wafer's position on refractive index measurement and thicknes...................................62
4.4.3 density of CVD deposited SiO_2 film (uniformity of film).......................66

5. CONCLUSIONS.......................................70

BIBLIOGRAPHY..71

List of figures

Figure 1. Hot-wall, low pressure Chemical Vapor Deposition reactor used for routine deposition. 2

Figure 2. Film growth rate as a function of temperature for a typical CVD process. 6

Figure 3. Deposition rate as a function of Diethylsilane flow rate for LPCVD deposited silicon dioxide from DES. 14

Figure 4. Deposition rate as a function of temperature for LPCVD deposited silicon dioxide from DES. 15

Figure 5. Various types of vibration in infrared spectra. 19

Figure 6. Infrared spectrum of vitreous quartz and thermal growth SiO_2 film. 20

Figure 7. A typical infrared spectrum with the Si substrate signal electronically subtracted. 21

Figure 8. Elements of Polarizer-Retarder-Sample-analyzer ellipsometer. 29

Figure 9. Absorbance of SiO_2 film (J31) with different thickness after each etching. 36

Figure 10. Infrared spectra of SiO_2 at different deposition temperature (A) J95, 375°, (B) J101, 475°C. 39

Figure 11. Infrared spectra of SiO_2 film deposited at 475°C. 41

Figure 12. Infrared spectra of SiO_2 film deposited at 375°C. 42

Figure 13. The Si-O-Si bonding arrangement. 44

Figure 14. Infrared spectra around 3u band for sample J101 (475°C deposited). 46

Figure 15. Infrared spectra around 3u band for sample J95 (375°C deposited). 47

Figure 16. The SiO_2 film thickness vs P-etch time for the DES flow rate series samples. 52

Figure 17. P-etch rate of silicon dioxide film plotted vs DES flow rates. 54

Figure 18. The SiO_2 film thickness vs P-etch time for the temperature series samples. 55

Figure 19. P-etch rate of SiO_2 film plotted as a function of deposition temperatures. 56

Figure 20. Effect of different annealing temperatures on etch rate of SiO_2 film (J95). 58

Figure 21. P-etch rate of silicon dioxide as a function of different measured temperatures. 61

Figure 22. Refractive index of silicon dioxide as a function of deposition temperatures. 64

Figure 23. Thickness profile of SiO_2 film (in horizontal direction). 68

Figure 24. Thickness profile of SiO_2 film (in vertical direction). 69

List of Tables

Table 1. Physical properties of silicon dioxide. 8

Table 2. SiO_2 thin film samples preparation conditions (Flow rate series) 13

Table 3. SiO_2 thin film samples preparation conditions (temperature series) 13

Table 4. Infrared spectral regions. 16

Table 5. Standard data of SiO_2 for the computer simulations 28

Table 6. Methods for thin film thickness measurements. 32

Table 7. Color Chart for SiO_2 films when observed perpendicularly under daylight fluorescent lighting. 33

Table 8. The annealing effects on infrared spectra of SiO_2 films deposited at different temperatures 40

Table 9. The heating effects on infrared spectra of SiO_2 films deposited at different DES flow rates 50

Table 10. Etch rates of SiO_2 films produced for various DES flow rates. 53

Table 11. Etch rates of SiO_2 films produced at various temperature. 57

Table 12. Effect of annealing temperatures on etch rate of SiO_2 films. 59

Table 13. Temperature effect of etch rate of silicon dioxide. 60

Table 14. The refractive index, thickness, and density of the SiO_2 film from run #25 as a function of wafer position. 65

1. INTRODUCTION OF CVD FILM

1.1 A REVIEW OF CVD TECHNIQUES

The most common technique for growing thin film of a wide variety of materials on various substrates [1], is chemical vapor deposition (CVD) [2]. This technique, first reported by Sangster [3] in 1957, has become the commercial technique for various thin film preparation.

Chemical vapor deposition is a process where one or more gaseous species react on a solid surface and one of the reaction products is a solid phase material.

When chemical vapor deposition was first used for polysilicon deposition, the most common CVD system was the horizontal, atmospheric-pressure reactor widely used in the late 1960s and early 1970s. This type of system allows operation over a wide temperature range, but its capacity is severely limited by the size of the susceptor on which the wafers are placed in a single layer. The low-pressure CVD (LPCVD) reactors, which were developed to overcome the limited capacity of the horizontal systems, can form thin films on 100-200 wafers simultaneously, although, the range of conditions over which it can operate satisfactorily is severely limited. The basic elements of the LPCVD reactor are illustrated in Figure 1.

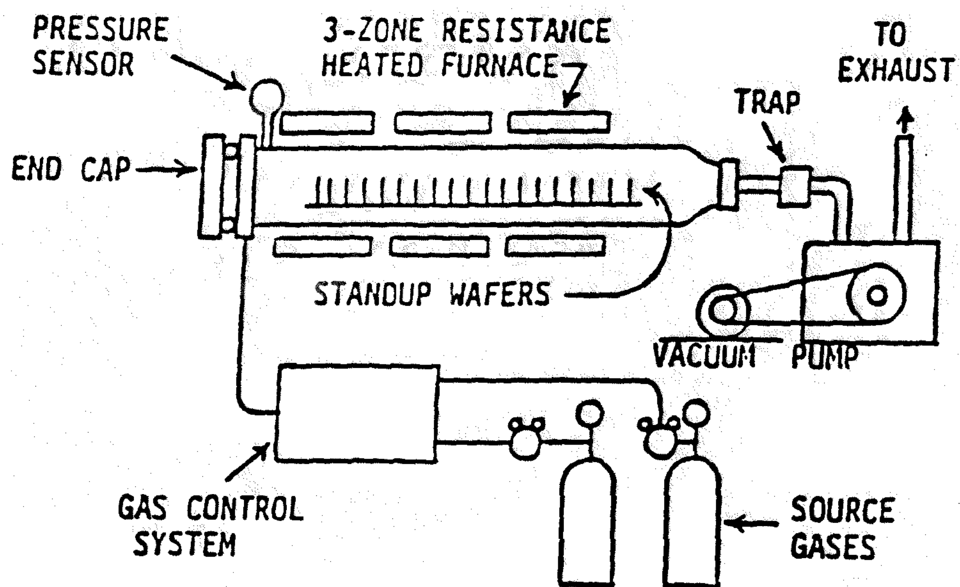

Figure 1. Hot-wall, low pressure Chemical Vapor Deposition reactor used for routine deposition [1].

1.2 FUNDAMENTAL OF LPCVD REACTION

There are several types of hot wall reactors which operating at low pressure (typically 0.1 - 10 torr) for LPCVD in the low-, mid-, or high-temperature ranges such as tubular (Figure 1), bell-jar, or close-spaced design. In the horizontal tubular design the substrate slices (silicon wafers) stand up in a carrier sled or boat and gas flow is horizontal. The reduced pressure increases the mean-free path of the reactant molecules, which allows a closely spaced wafer stacking.

CVD is a heterogeneous reaction involving at least the following steps:

I. Arrival,

1. bulk transport of reactants into the process volume,
2. gaseous diffusion of reactants to the surface,
3. absorption of reactants onto the surface,

II. Surface reaction,

4. surface reaction (reaction can also take place in the gas volume immediately above the surface),
5. surface diffusion,

III. Removal of reactant by-products,

6. reaction by-product desorption,
7. gaseous transport of by-products,

8. bulk transport of by-products out of process volume.

The rate of chemical vapor deposition is primarily controlled by one of the following major groups of process steps:

* The rate of arrival of reactants,
* The surface reaction rate,
* The rate of removal of by-products.

When the surface reaction rate controls the process, the overall reaction rate can be written as

$$R = Ck = Ck_0 \exp(-E_a/kT)$$

where the reaction-rate coefficient k is characterized by an apparent activation energy E_a, and C is a proportionality constant.

Either diffusion through the boundary layer or reaction at the surface of the wafer may limit the overall deposition process. Gas-phase diffusion varies only slowly with temperature, increasing as $T^{1.5}$ or T^2, while a reaction rate increases rapidly with temperature increasing, varying as $\exp(-E_a/kT)$. At higher temperatures, the reaction proceeds rapidly, and diffusion of the gaseous silicon species through the boundary layer to the wafer surface limits the overall deposition process. In this mass-reaction-limited regime of operation, the deposition rate is only a weak function of temperature. As the temperature is reduced, the reaction rate decreases rapidly until it becomes the

limiting step in the overall deposition process. In the surface-reaction-limited regime of operation, the deposition rate is a strong function of temperature (Figure 2.). The excellent temperature control is needed in this operating regime to achieve the film thickness uniformity required for controllable integrated-circuit fabrication. Depending on the substrate temperature, temperature gradient of the reaction tube, concentration (flow rate), composition and pressure of the reaction agent, diameter and length of the reaction tube, etc, deposition of the thin film process can be controlled.

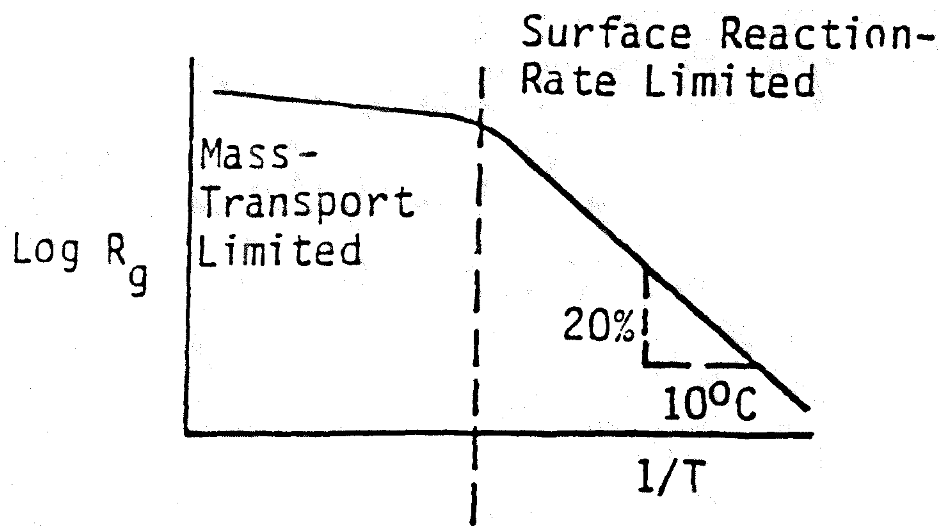

Figure 2. Film growth rate as a function of temperature for a typical CVD process [2].

2. LPCVD DEPOSITED SILICON DIOXIDE (SiO_2) FILM

2.1 APPLICATION OF SiO_2 THIN FILM

Silicon dioxide has played an important role throughout the development and fabrication of semiconductor microcircuits over the years. Its major functions have been for insulating circuit elements, serving as material for storage capacitors, passivating and protecting device surfaces, and insulating double-level conductor lines.

Because of its unexcelled purity and outstanding dielectric of interface properties, silicon dioxide thin film is one of the most important dielectric-film materials deposited by CVD which meets the requirements of the very large scale integrated (VLSI) technique. Silicon dioxide can be deposited by CVD at a low enough temperature to preserve the final metallization.

SiO_2 has gained its importance for practical applications by the fact that it is the only substance with which hard and stable layers with a refractive index < 1.5 can be obtained [4]. The physical properties of SiO_2 are given in Table 1.

Table 1.Physical properties of silicon dioxide.[6]

melting point	1500°C
boiling point	2950°C
Heat cap.,cal/g 100°C	0.185
Si-O distance,A	1.62
Density,g/cm^3, 0°	2.1975
Mohns hardness	7.7
index refr. 5893A	1.4584
Young's Modules	10.5 x 10^6 Psi [29]

2.2 LOW-TEMPERATURE DEPOSITED SILICON DIOXIDE THIN FILM

Historically, silicon dioxide formed by thermal oxidation of the silicon substrate has been used as the dielectric and insulator material on silicon device technology. The processing temperature of thermal growth SiO_2 is in the range of 1000 -1200°C. Low-temperature deposition of SiO_2 thin films is of considerable interest to current very large scale integrated (VLSI) technology. As metal oxide semi-conductor devices are reduced in size to increase density and performance, device processing temperatures become even more important.

Probably the most widespread method for depositing low-temperature CVD oxides is the controlled oxidation of silane (SiH_4) first introduced in the literature by Goldsmith and Kern in 1967 [5]. To prevent premature oxidation, the silane was diluted with an inert carrier gas in the reaction chamber. Using this technique, Goldsmith and Kern obtained SiO_2 films at temperatures ranging from 250° to 550°C, with most work in the 400° - 450°C temperature range.

2.3. NEW CHEMICAL SOURCE OF CVD DEPOSITED SiO_2 THIN FILMS

However, SiH_4 is a toxic, pyrophoric, and potentially explosive gas which requires expensive installations to meet the safety standards.

Over the past decades a great effort has been made to investigate a suitable compound for depositing SiO_2 thin films at low temperature, not only for safety, but also for minimizing the problems of junction element and overcoming thickness limitations.

Various chemical sources and deposition methods for CVD deposited SiO_2 thin films have been used by different workers: thermal decomposition of Ethyl-triethoxy-silane $(CH_3CH_2)-Si(OCH_2CH_3)_3$ [7]; Vinyl-triethoxy-silane $CH_3=CHSi(OCH_2CH_3)_3$; Phenyl-triethoxy-silane $C_6H_5Si(OCH_2CH_3)_3$; Amyl-triethoxy-silane $C_5H_{11}Si(OCH_2CH_3)_3$; Diphenyl-diethoxy-silane $(C_6H_5)_2-Si(OCH_2CH_3)_2$; Dimethyl-diethoxy-silane $(CH_3)_2Si(OCH_2CH_3)_2$ [8]; Tetroethoxy-silane $Si(OCH_2CH_3)_4$ [8,9]; and recently, Mono-alkyl cyclic siloxane; 2,4,6,8-tetra-methyl-cyclotetrosiloxane [9]; Tetrabutoxy-silane, and tetrapropoxy-silane [10].

The new liquid chemical source that was used for deposition SiO_2 thin films in this work is Diethylsilane $(C_2H_5)_2SiH_2$ (DES). The ratio of silicon to carbon is 0.25 for DES, the boiling point is 56^oC, and the outstanding advantage of this material is high vapor pressure, 200 Torr at close to room temperature (21°C). It is a non-pyrophoric and non-toxic material and therefore to safe use.

3. CHARACTERIZATION OF SiO_2 FILM

3.1 INTRODUCTION

This work is concentrated on the evaluation of LPCVD deposited SiO_2 thin film with DES as a chemical source. CVD deposited SiO_2 thin films are evaluated for, density, porosity, annealing effects on bond strain, refractive index, and thickness. This chapter introduces the techniques for the evaluation of above mentioned parameters. The techniques included the use of infrared absorption spectroscopy, P-etch procedures [12], optical measurement of refractive index and thickness [13]. Thermal annealing of CVD films in a vacuum ambient has been proposed to improve oxide quality.

The CVD silicon dioxide thin film is grown on a clean silicon wafer by reacting DES and oxygen gas at a temperature about 450°C. As illustrated in Figure 1, in the experimental reactor, the reactor chamber consists of a 19.1 cm inner diameter quarts tube in a 155 cm long five heating zoned, Lindberg furnace. At one end liquid source can injected from a glass bubbler into the reaction chamber. For the injection system, due to the pressure differential between the bubbler (containing DES liquid) and the vacuum chamber, the evaporated gas passes through the mass flow

controller into the reaction chamber. Oxygen flow into the reaction chamber is controlled by a mass flow controller. Edwards High Vacuum Pump with a Mechanical Booster Drive is used to create the necessary vacuum in the system. Two cooling fans were installed at both ends of chamber to avoid overheating of O-ring.

The properties of the CVD thin film are dependent on the deposition conditions and the reactor. The characterized CVD deposited silicon dioxide samples are included in two series:

i. DES flow rate series:

The SiO_2 films were deposited at various DES flow rate from 20 to 150 sccm, a ratio of O_2 to DES of 2, a pressure of 0.5 Torr, and a temperature of 450°C.

ii. Deposition temperature series:

The silicon dioxide films were prepared by various temperature from 375° to 475°C, a ratio of O_2 to DES of 2, a pressure of 0.5 Torr, and a constant DES flow rate of 50 sccm.

The details information of the CVD SiO_2 thin film preparation are given in table 2 and table 3.

The relation between SiO_2 deposition rate in A/min and the flow rate of DES is given in Figure 3. The almost linear dependence of logarithm deposition rate of CVD SiO_2 with deposition temperature is given in Figure 4.

Table 2. SiO_2 thin film samples preparation conditions (Flow rate series)

sample ID #	condition of deposition				deposition rate (mg/hr.)
	temp °C	ratio O_2/DES	flow rate DES(sccm)	pressure (Torr)	
J74	450	2	150	0.5	18.9
J65	450	2	120	0.5 *	21.6
J44	450	2	100	0.5	13.1
J60	450	2	85	0.5	13.8
J47	450	2	65	0.5	10.8
J52	450	2	50	0.5	9.7
J40	450	2	35	0.5 *	14.0
J56	450	2	20	0.5	8.8

* Double side deposition

The rest are single side deposition. Those were made by back to back side of wafer.

Table 3. SiO_2 thin films samples preparation conditions (temperature series)

sample ID #	condition of deposition				deposition rate (mg/hr.)
	temp °C	ratio O_2/DES	flow rate DES(sccm)	pressure (Torr)	
J95	375	2	50	0.5	6.3
J92	400	2	50	0.5	8.7
J98	425	2	50	0.5	10.8
J104	450	2	50	0.5	14.5
J101	475	2	50	0.5	15.2

All of silicon dioxide samples which list in this table are double side deposition.

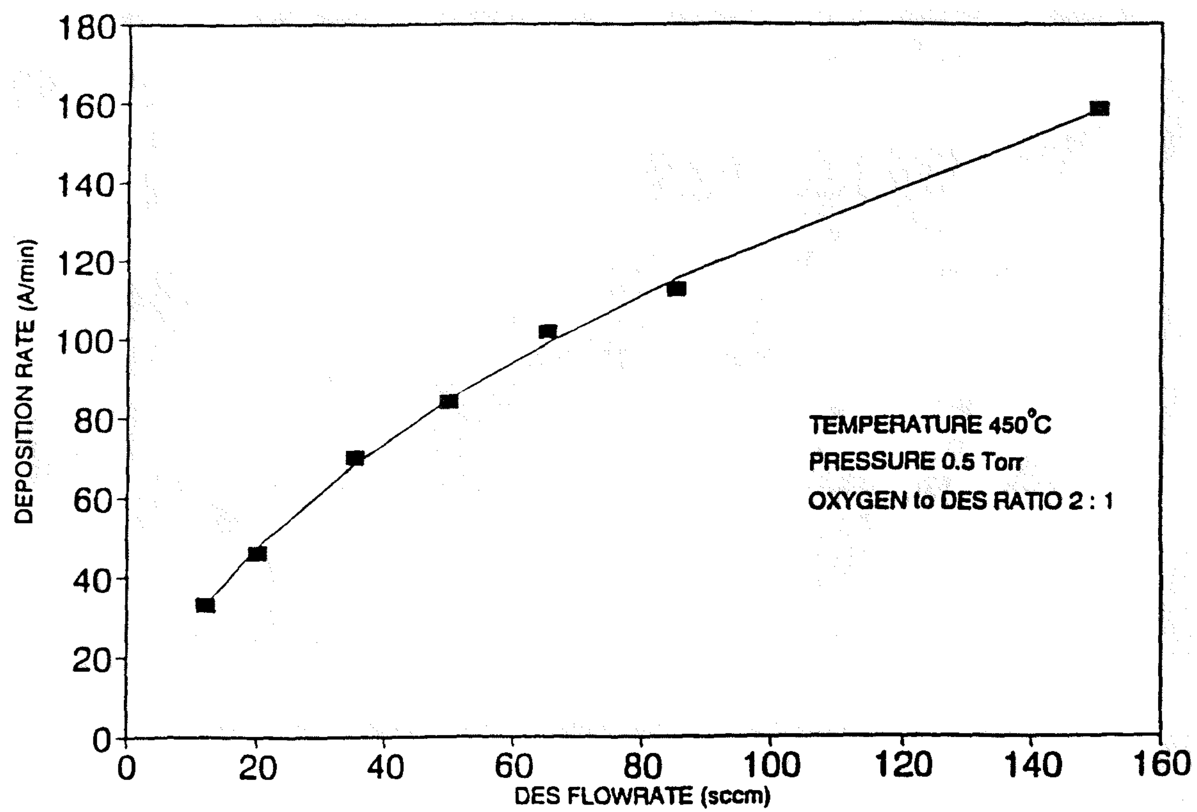

Figure 3. Deposition rate as a function of Diethylsilane flow rate for LPCVD deposited Silicon dioxide from DES [11].

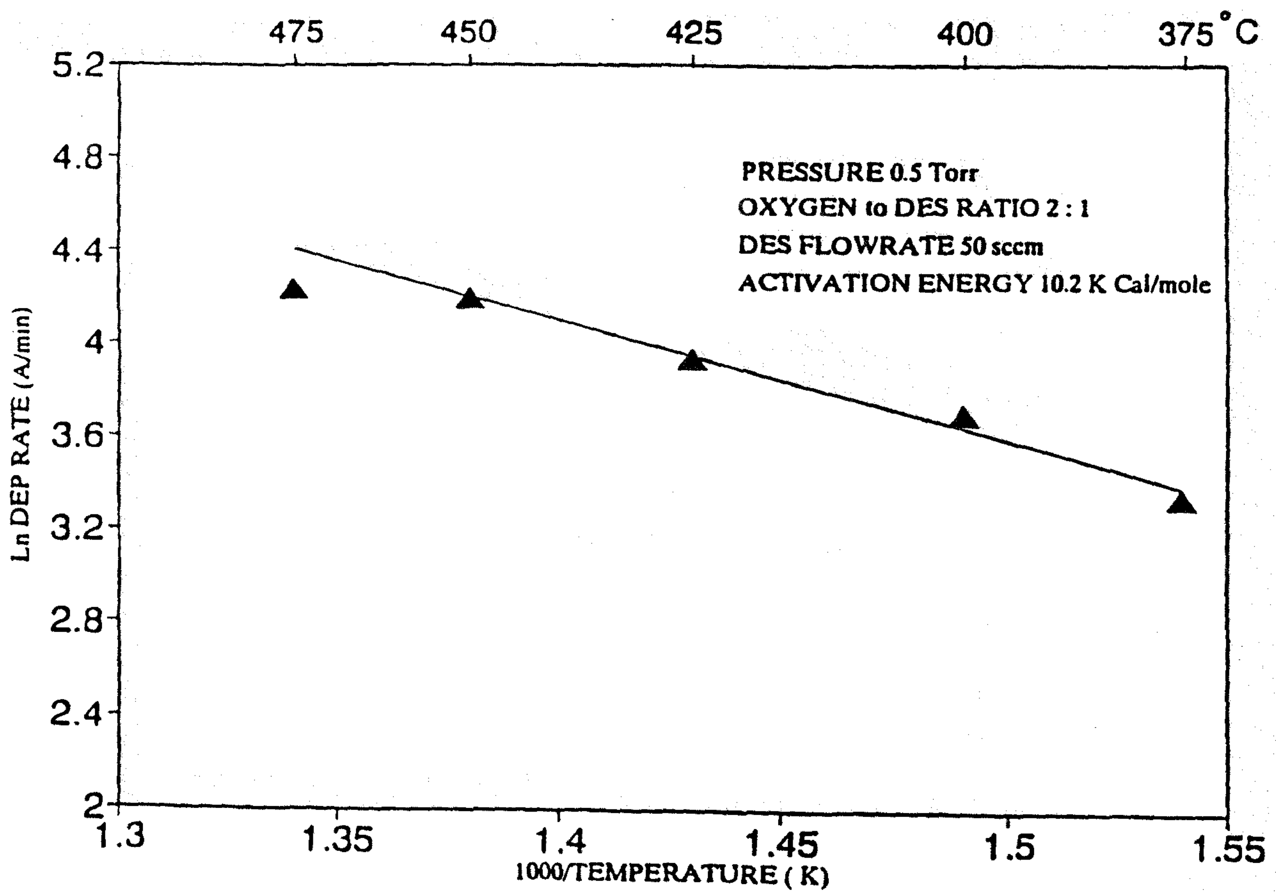

Figure 4. Silicon dioxide film Deposition rate as a function of temperature for LPCVD deposited silicon dioxide from DES [11].

3.2 INFRARED SPECTROSCOPY

3.2.1 Introduction of infrared spectroscopy

The infrared region of the spectrum encompasses radiation with wavenumbers ranging from about 12,800 to 10 cm^{-1} or wavelengths from 0.78 to 1000 *um*. From the stand-point of both application and instrumentation, it is convenient to subdivide the spectrum into *near-*, *middle-*, and *far-*infrared radiation; rough limits of each are shown in Table 4. The majority of analytical applications are confined to a portion of the middles region extending from 4000 to 400 cm^{-1} or 2.5 to 25 *um*.

Table 4 . Infrared spectral regions.

Region	wavelength (λ) Range, um	Wavenumber (σ) Range, cm^{-1}	Frequency (ν) Range, Hz
Near	0.78 to 2.5	12800 to 4000	$3.8x10^{14}$ to $1.2x10^{14}$
Middle	2.5 to 50	4000 to 200	$1.2x10^{14}$ to $6.0x10^{12}$
Far	50 to 1000	200 to 10	$6.0x10^{12}$ to $3.0x10^{11}$
Most used	2.5 to 15	4000 to 670	$1.2x10^{14}$ to $2.0x10^{13}$

In order to absorb infrared radiation [14], a molecule must undergo a net change on dipole moment as a consequence of its vibrational motion. Only under these circumstance can the alternating electrical field of the radiation interact with the molecule and cause changes in the amplitude of its motion. The dipole moment is determined by the magnitude of the charge and the distance between the two centers of charge.

There are basically two kinds of vibrations: *Stretching* and *bending*. A stretching vibration involves a continuous change on the interatomic distance along the axis of the bond between two atoms. Bending vibrations are characterized by a change in the angle between two bonds and are of four types: scissoring, rocking, wagging, and twisting. The various types of vibrations are shown schematically in Figure 5.

3.2.2 The application of the infrared spectroscopy in SiO_2 thin film

Infrared spectroscopy is a very useful technique which can determine the chemical nature of a thin film. The absorption band intensities of transmitted spectra are roughly proportional to the film thickness, i.e, they obey Beer's law well and are much better for qualitative determinations than reflection spectra.

When infrared radiation of a particular frequency is passed through a sample containing molecular species, it may or may not be absorbed. If all frequencies are passed through, each will be absorbed to varying degrees, depending on the molecular species involved.

As an example in Wong's early work [15], a typical spectrum of absorbance versus wave number (cm^{-1}) (wave number = 1/wavelength) for both vitreous quartz and thermal growth silicon dioxide thin film is illustrated in Figure 6. The thermal growth silicon dioxide (1000° -1200°C) is formed by the oxidation of the silicon itself [16]. This oxide is very reproducible and very stable chemically under controlled oxidation conditions. The infrared spectra of thermal oxide serves as a standard by comparing of band position (indicating the difference of dense and bond angle of Si-O-Si) and band intensity (to be proportional to the thickness of the film) of SiO_2 deposited by other techniques. The 1080 cm^{-1} absorption band in Figure 6 used for quantitative analysis arise from the vibration of Si-O-Si for thermal growth silicon dioxide. The shifting of this band indicates the dense changing of SiO_2 (higher frequency is contributed by more dense and large Si-O-Si bond angle than lower frequency). It can be seen in Figure 7, that other absorption bands for SiO_2 at ~ 800 cm^{-1} and 460 cm^{-1}, as indicated by Kobeda, Kellam and Psburn [17], are an in plane bending and an out-of-plane rocking vibration respectively.

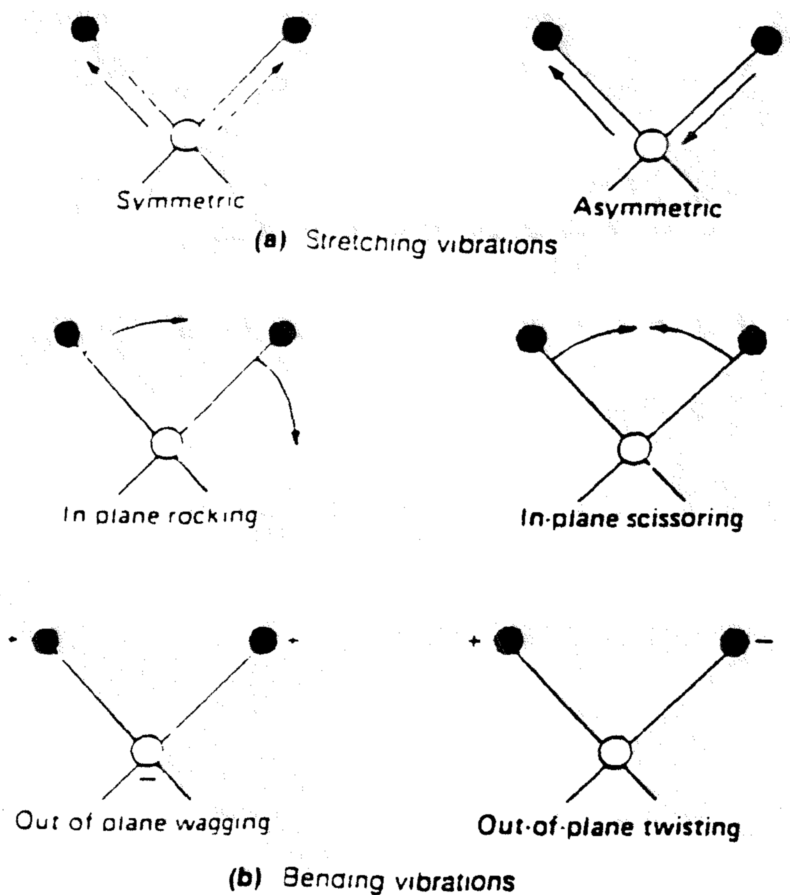

Figure 5. various types of vibration in infrared spectra. Note: + indicates motion from the page toward the reader; - indicates motion away from the reader [14].

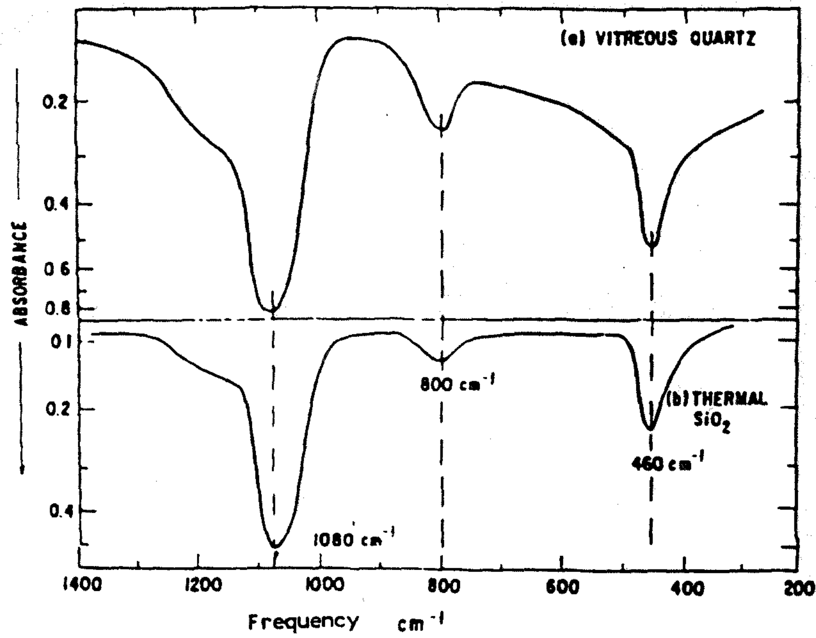

Figure 6. Infrared spectrum of vitreous quartz and thermal growth SiO_2 film [15].

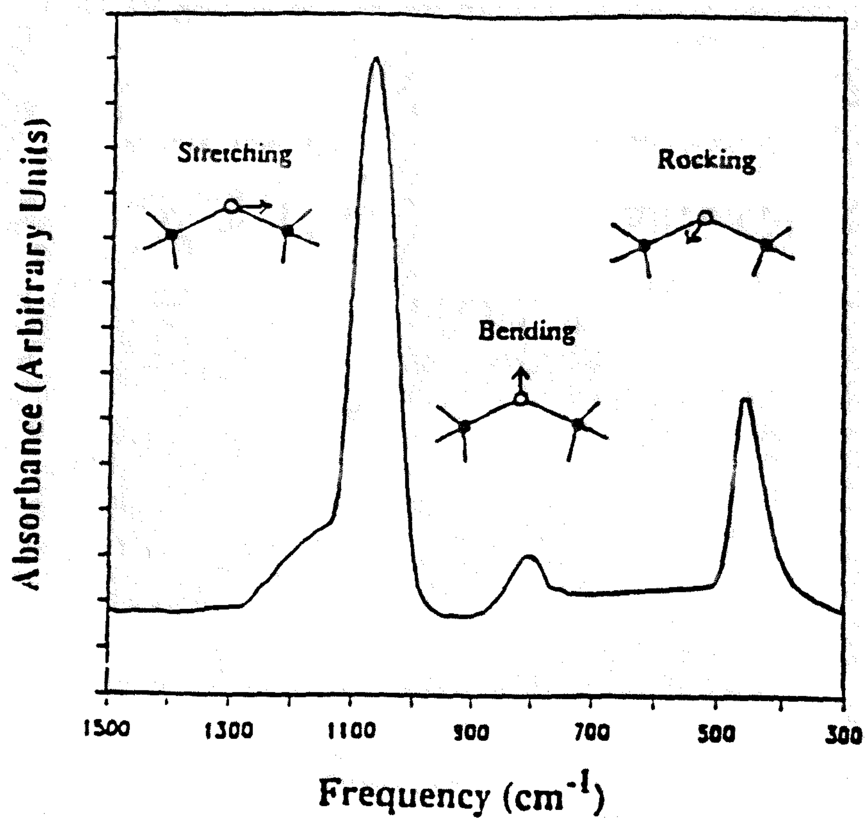

Figure 7. A typical infrared spectrum with the Si substrate signal electronically subtracted. The dark circles represent Si and the light circles oxygen [17].

3.3 CHEMICAL ETCH TECHNIQUES

3.3.1 Introduction of wet etching

Wet etching has played an important role in semiconductor fabrication from the very beginning of this technology, because it is fast, simple, and convenient. In recent years, with the advent of plasma etching as the emerging technology, wet etching has been relegated to secondary status in spite of the fact that it remains the 1st widely-used etching process [18].

3.3.2 Basic etching theory

There are four main types of etching precesses:

I. Dissolution:

The dissolving of a material in a liquid solvent without any change in the chemical nature of the dissolved specie (not a very prevalent practical etch).

II. Oxidation-Reduction (Redox):

This is the conversion of material to a soluble higher-oxidation state,

Example: $m \rightarrow m^{n+} + ne^{-}$ (1)

These reaction may occur in a completely chemical system through the use of an oxidizing agent, or in an

electrochemical cell.

III. Complexation:

This is a common reaction with oxidation-reaction ligand groups (an atom or group of atoms which donates a pair of electrons to a central atom forming a bond) surround and bond chemically to the etched species forming a soluble complex, ion , or molecule.

IV. Gas phase:

Involves the vaporization of the etchant in a vacuum or inert atmosphere, usually at high temperature. The vapor reacts with the surface to be etched to produce volatile products.

3.3.3 Chemical etching SiO_2

The amorphous nature of SiO_2 causes etch rates to be nondirectional. SiO_2 etching is accomplished by HF and fluorine ions in solution. The typical reaction is as follows [19]:

$$SiO_2 + 6HF \Leftrightarrow H_2SiF_6 + 2H_2O \qquad (2)$$

Going through the literature in 1960s and 1970s, many papers have published about SiO_2 wet etching. Most evaluation work have done for SiO_2 film with comparing the different deposition processing. The various etchants have been employed for different processed SiO_2 film. There are the different concentrated HF solution [20,21,22,23],

buffered HF solution (the addition of NHF_4 to HF is called buffering and the resulting solution is buffered HF) [20, 23, 24, 25, 26] and P-etch [20, 12, 27, 28, 29, 30] etchants for SiO_2 etching studies.

3.3.4 P-etch for SiO_2 thin film

The first step in selecting an oxide etch process is to define the goals for the process. Determine what range of oxide thickness desired. With these goals in mind it becomes relatively easy to select a process. In this work the purpose is to remove the controllable very thin layers of SiO_2. In order to evaluate the SiO_2 films with different deposition conditions, a lower etch rate is necessary. In literature the data show us that for thermal growth SiO_2, the etch rate is about 5000 A/min. in concentrated HF solution[22], 1000 A/min. in buffered HF [25], and 125 A/min. [30] in P-etch solution; for different processes CVD SiO_2 films, the P-etch rate in the range of 800 to 950 A/min [22, 30]. In this work the thickness of the SiO_2 film which prepared with the different condition in the range of 3000 to 7000 angstrom (A), the P-etch should be the good choice for this study.

The selected P-etch solution [6] consists of 15 parts hydrofluoric acid (49%), 10 parts nitric acid (70%), and 300 parts water.

3.4 THERMAL ANNEALING

3.4.1 Introduction of thermal annealing

In general, dielectric films such as SiO_2 deposited in CVD processes are amorphous films. For a comparison with the thermal growth silicon dioxide films, the thermal annealing technique has been used for improving the silicon dioxide quality films. The densified silicon dioxide films which were deposited at different conditions are compared with thermal growth silicon dioxide films in order to determine the extent of densification.

The films can be densified by short term exposure in different ambients (steam, various dry gases, or vacuum) at varies temperatures. The steam is more effective for densification than dry gases and vacuum. P-etch rate of silicon dioxide shows initially that deposited film is much faster than that exposed at high temperature [30].

3.4.2 The thermal annealing of SiO_2

Generally, the densified process results in increasing refractive index, decreasing the P-etch rate, and decreasing film thickness. Infrared spectra of the densified SiO_2 film show a shifting of strong stretching Si-O-Si band (~ 1070 cm^{-1}) to higher frequency and decrease in band width after

densification [30]. As previous mentioned this is the results of the more dense film and the strain of the bond. The degree of band shifting of SiO_2 film depends on the deposition and annealing temperature.

3.5 REFRACTIVE INDEX, ELLIPSOMETRY

3.5.1 Introduction of ellipsometric technique

During the past decades, ellipsometry acquired increasing importance in industrial areas, particularly in the technology of microelectronic devices.

Most application of ellipsometry in the technology of microelectronic devices comprise the investigation of thin insulating films, usually on semiconductor substrates. For a variety of industrially used substrate-film systems, ellipsometry becomes one of the standard analytic techniques. Aside from thermally grown or anodic oxides, these films are usually deposited by plasma enhanced oxidation or deposition, or by chemical vapor deposition. These processes are generally established although effort is still required to fully understand the dynamics of the mechanisms involved in some of them.

3.5.2 Basic physics of ellipsometry

Ellipsometry is a technique for the contact-less and

non-destructive optical characterization of surfaces [31]. It is based on the fact that a monochromatic electromagnetic wave changes its state of polarization if it strikes nonperpendicularly the interface between two dielectric media.

The ellipsometer creates an elliptically polarized monochromatic light beam, and then evaluates the light beam on reflection from a thin film. The essential ingredients from an ellipsometer are shown in Figure 8. A monochromatic beam of light passes into a polarizer where it becomes plane polarized. It then passes through a compensator which converts it into an elliptically polarized light beam. After reflection from the substrate-thin film, it passes through an analyzer. If it had been converted back to plane polarized when it had been reflected, then it would be possible to rotate the analyzer to find a true minimum intensity. The technique then is rotated to determine the position corresponding to a minimum in light intensity. The pair azimuth angles are: the polarizer P, and the analyzer A. These two scalar ellipsometric angles obtained from one ellipsometric measurement permit the calculation of two independent scalar parameters of the sample. The calculation from P and A results in psi and delta. The subsequent analysis of psi and delta makes the actual determination of the sample parameters.

The parameters determined most frequently in technical

tronics, are the thickness and the refractive index of a thin dielectric or slightly absorbing film on a substrate with known properties. The refractive index of the film renders valuable information about the film composition or structure. Ellipsometry is the only technique which within a certain thickness range (particularly for films in the thickness region of a few hundred nanometers or less).

A computer program simulation is available to ellipsometric measurement. Although, details of the computer simulation will not be discussed here. This simulations is essentially based on the data of the system silicon-SiO_2-air and the necessary data P & A was input with the thickness and the refractive index of the film output. The following parameters (Table 5.) were used in the simulations.

Table 5. Standard data for the computer simulations [29]

Ellipsometer:	PRSA null ellipsometer
Wavelength:	λ = 632.8 nm
Angle of incidence:	a = 70°
Retarder:	ideal quarter-wave plate
Transmittance ratio:	T_c = 1
Phase shift:	Δ_c = 90°
Azimuth medium:	Q = - 45°
Immersion medium:	air (n_m = 1)
film medium	SiO_2 (n_f = 1.45)
Substrate medium:	Silicon (n_s = 3.85)

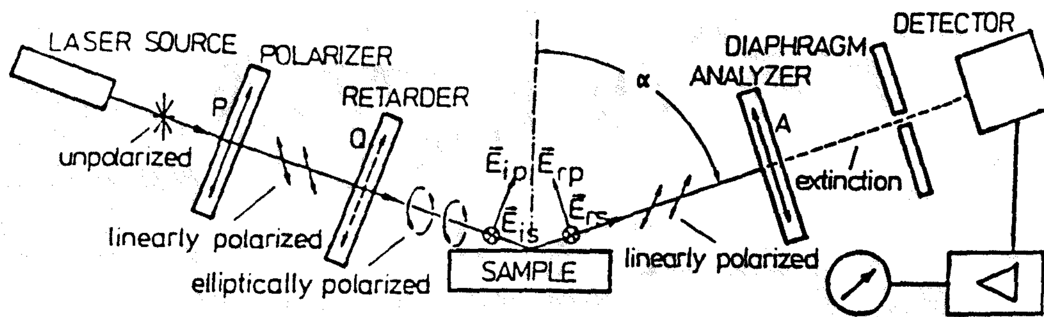

Figure 8. Elements of PRSA (Polarizer-Retarder-Sample-analyzer) ellipsometer [29].

3.5.3 Refractive index measurement of silicon dioxide films

The measurement of refractive index was accomplished by using two instruments: The refractive indices of temperature series sample were carried out by using Rodolph Ellipsometer (The wavelength is 6328A). Others measurements were measured by using Thin Film Ellipsometer, type 43603-200E, Ser No. 5093, RuDolph Research Flander, NJ. The mercury light as a light source with the wavelength 5461 A.

3.6 THICKNESS MEASUREMENT

3.6.1 The introduction of thin film thickness measurement method

Thickness measurements are important because depths of the various films combined in an electronic device determine many of its operating characteristics. Table 6 lists various methods in common use for determining thickness.

The measurement of film thickness can be fairly simple measurement or quite complex, depending on the nature of the film. A very thin film on a dielectric substrate may be scanned by visible light [32].

In addition, the relative magnitude of the index of refraction of film and substrate is important [33]. If transmittance is observed for $n_f > n_s$ at a given wavelength

with increasing film thickness (here n_f, n_s is refractive index of the film and the substrate respectively), it will at first be found to decrease, reaching a minimum at a thickness value which corresponds to $\lambda/4$ of the light used for the investigation (here λ is wavelength). Then the transmittance will increase up to a maximum at $\lambda/2$, and so on; i.e., maxima will be found at "optical thickness" nt = m $\lambda/2$, and minima will occur for nt = $(2m + 1)\lambda/4$ (t is the physical film thickness, n is the index of refraction, and m is an integer). The position of maxima and minima is reversed if the reflectance is measured. The sequence for occurrence of maxima and minima is also reversed for $n_f < n_s$ as compared with $n_f > n_s$. This averaging technique requires that light be transmitted through the sample and neglected multiple reflection.

3.6.2 Silicon dioxide thin film thickness measurement

Optical techniques are available for thickness evaluation of SiO_2 thin film on silicon. The interference of a nonabsorbable materials on a dielectric substrate shows a color effect. The color of a thin film could be correlated to its thickness (as SiO_2 on silicon in table 7) [13]. In fact, one of the more useful aspects of this technique is that one can make rapid judgements as to film uniformity.

Table 6. Various methods for thin film thickness measurement [30]

I DESTRUCTIVE METHODS	A. Step height 1. Interferometry: a. Single beam b. Multiple beam B. Sectioning : 1. Angle lap and stain 2. Grooving 3. Cleaving along crystal planes
II NON-DESTRUCTIVE METHODS	A. Mechanical: 1. Weight difference 2. Electronic thickness gauge 3. Stylus techniques B. Optical: 1. Stacking faults 2. Infrared reflection 3. Optical density 4. Reflection: a. X-ray b. Beta ray 5. Ellipsometry 6. Frustrated total internal reflection 7. Variable angle monochromatic fringe observation 8. Step gauge color comparison C. Electrical: 1. Frequency change of quartz crystal oscillations 2. Change of resistivity, Hall mobility Hall constant, etc. 3. Eddy current methods
III METALLIC TESTS MAGNETIC METHODS	A. Force of attraction B. Parallel flux C. Transformer principle

Table 7. Color Chart for SiO_2 films observed perpendicularly under daylight fluorescent lighting [13].

Film Thickness (microns)	*Order (5450 A)*	*Color and Comments*
0.05$_0$		Tan
0.07$_5$		Brown
0.10$_0$		Dark violet to red-violet
0.12$_0$		Royal blue
0.15$_0$		Light blue to metallic blue
0.17$_5$	I	Metallic to very light yellow-green
0.20$_0$		Light gold or yellow—slightly metallic
0.22$_5$		Gold with slight yellow-orange
0.25$_0$		Orange to melon
0.27$_5$		Red-violet
0.30$_0$		Blue to violet-blue
0.31$_0$		Blue
0.32$_5$		Blue to blue-green
0.34$_5$		Light green
0.35$_0$		Green to yellow-green
0.36$_5$	II	Yellow-green
0.37$_5$		Green-yellow
0.39		Yellow
0.41$_2$		Light orange
0.42$_6$		Carnation pink
0.44$_3$		Violet-red
0.46$_5$		Red-violet
0.47$_6$		Violet
0.48$_0$		Blue-violet
0.49$_3$		Blue
0.50$_2$		Blue-green
0.52$_0$		Green (broad)
0.54$_0$		Yellow-green
0.56	III	Green-yellow
0.57$_4$		Yellow to "yellowish." (Not yellow but is in the position where yellow is to be expected. At times it appears to be light creamy grey or metallic.)
0.58$_5$		Light-orange or yellow to pink borderline
0.60$_0$		Carnation pink
0.63$_0$		Violet-red
0.68		"Bluish." (Not blue but borderline between violet and blue green. It appears more like a mixture between violet-red and blue green and over-all looks greyish)
0.72	IV	Blue-green to green (quite broad
0.77		"Yellowish"
0.80		Orange (rather broad for orange
0.82		Salmon
0.85		Dull, light red-violet
0.86		Violet
0.87		Blue-violet
0.89		Blue
0.92	V	Blue-green
0.95		Dull yellow-green
0.97		Yellow to "yellowish"
0.99		Orange
1.00		Carnation pink
1.02		Violet-red
1.05		Red-violet
1.06		Violet
1.07		Blue-violet
1.10		Green
1.11		Yellow-green
1.12	VI	Green
1.18		Violet
1.19		Red-violet
1.21		Violet-red
1.24		Carnation pink to salmon
1.25		Orange
1.28		"Yellowish"
1.32	VII	Sky blue to green-blue
1.40		Orange
1.45		Violet
1.46		Blue-violet
1.50	VIII	Blue
1.54		Dull yellow-green

4. EXPERIMENTAL RESULTS AND DISCUSSION

4.1 INTRODUCTION

The experimental results of the characterization SiO_2 thin films are given in this chapter: in section 4.2 is the investigation of SiO_2 infrared spectroscopy ; in section 4.3 is etching rate study of silicon dioxide and refractive indices measurement of SiO_2 is discussed in section 4.4.

4.2 INFRARED SPECTROSCOPY

The quality of the thin film is strongly influenced by the deposition conditions such as deposition temperature, deposition rate, flow rate of chemical source, ratio of oxygen with DES, total pressure, type of reaction and etc. The porosity and the strain in the films will result in differences in the infrared spectra from the spectra obtained for thermal growth silicon dioxide.

In this study the infrared absorption characteristics of all SiO_2 films samples were investigated by using a Perkin-Elmer 580 double-beam grating Infrared Spectrophotometer. In all cases, a new silicon wafer of the same thickness and of the same crystal orientation as the sample was placed in the reference beam to eliminate substrate

absorption bands.

4.2.1 Effect of thickness on Si-O-Si absorption band

The infrared absorption, band position and intensity is a function of the thickness of the SiO_2 thin film. The sample (J-31) was deposited at the flow rate of DES is 30 sccm, a ratio of O_2 to DES of 2, a pressure of 0.5 torr and a temperature of 450°C. The infrared spectra of J31 with different thickness are given in Figure 9. The spectra were taken after each etching at room temperature, which removed a thinner layer of film. The number on the curve indicated how many times of etching test. The thickness after each etching was determined by NanoSpec/AFT200 (see detailed at section 3.6, page 30). The data of thickness after each etching are given in the Left corner of Figure 9.

From figure 9 it can confirm that the absorbed intensity decrease with the thickness decreasing, the band shift slightly to lower frequency, and the band width at half height decreasing. If only if there is no structure change.

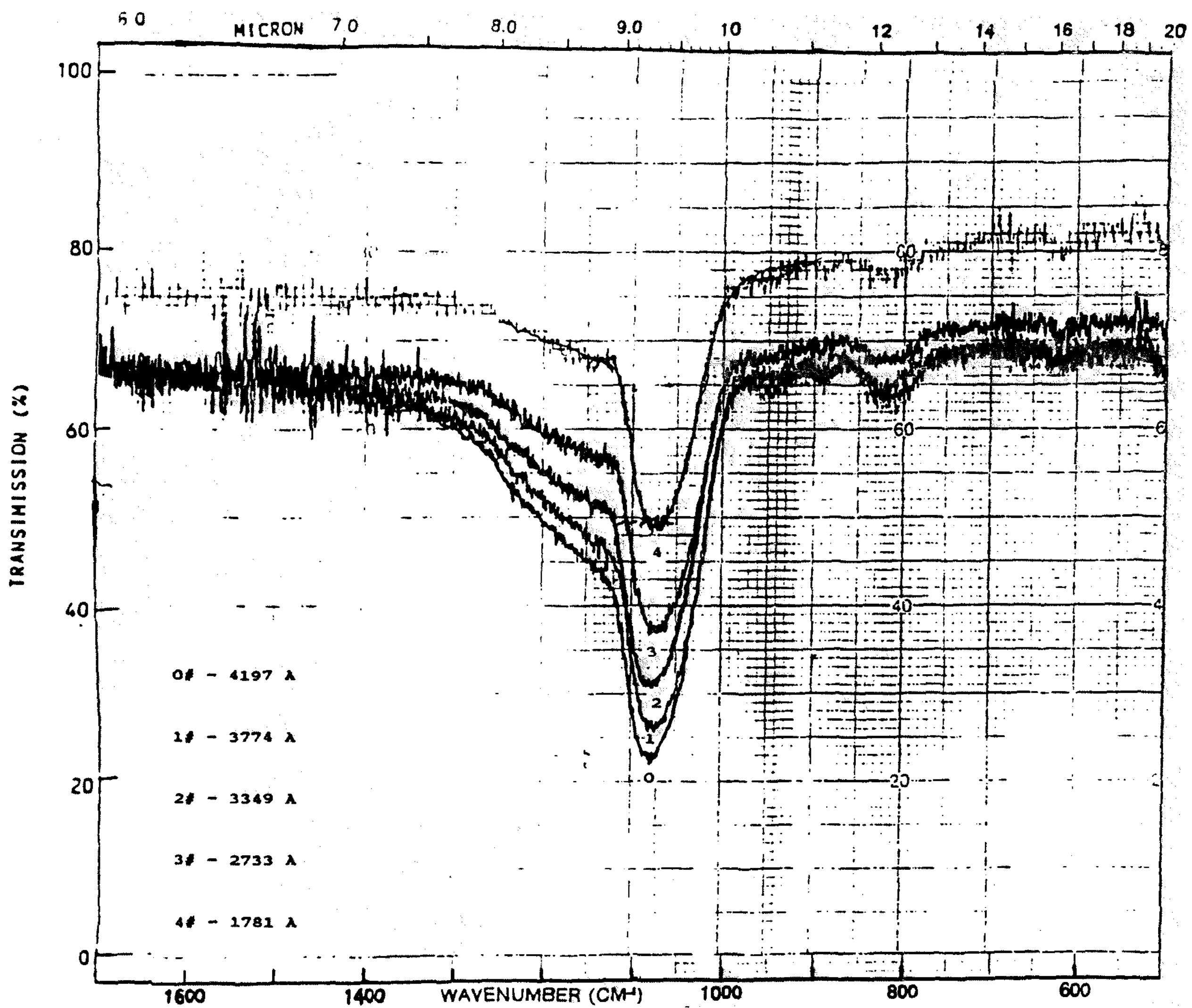

Figure 9. Absorbance of SiO_2 film (J31) with different thickness after each etching, the number on the spectra indicated times of etching.

4.2.2 Effect of deposition temperature on absorption band

Two samples (J95 and J101, thickness is 4461 A and 5380 A respectively) were deposited at 375° and 475°C respectively, the other parameters were kept the same (see detailed in Table 3., page 13). However as shown in Figure 10, the infrared spectra have distinguishable difference. For these two samples, the strong stretching band is 1068 cm^{-1} and 1075 cm^{-1} respectively, and the bending band is 819 and 815 cm^{-1} respectively. Due to the lower deposition temperature at 375°C, the 1070 cm^{-1} band is broad and shifted to lower frequency (1068 cm^{-1}), whereas the bending band at 800cm^{-1} is shifted to a high frequency. The band width at half height of sample J95 and J101 are 123 and 113 cm^{-1} respectively. In comparing CVD deposited silicon dioxide film with thermal oxides, which the stretching band is at a frequency of 1080 cm^{-1} [15] (Figure 6, page 20). The band positions in the spectra of silicon dioxide film are a function of porosity and strain. Lower temperature deposited CVD silicon dioxide (J95) somewhat porous film shows greater difference of the band position with thermal dioxide than the higher temperature deposited film. The band of higher temperature deposited film (J101) is sharper than lower temperature deposited film (J95). This results is agreement with Pliskin's study [18]. It should be noted that both the

band positions and half widths of thermal oxide vary slightly with thickness [32].

4.2.3 effect of annealing temperature on SiO_2 thin film quality

In this study, the annealing of the selected silicon dioxide samples from the flow rate series and deposition temperature series (refer Table 2 and Table 3) was carried out in a vacuum at temperatures of 600°, 750°, and 900°C respectively. The infrared spectroscopy, P-etch rate and refractive index measurement of these samples were performed after annealing. The discussion of the results in this section has been separated into three parts:

i. The annealing effect on the stretching and bending vibration of the SiO_2 thin film.

ii. The annealing effect on 3 um band of infrared spectra

iii. The annealing effect on the weak band at the frequency of 890 cm^{-1}.

i. The annealing effect on the mainly stretching and bending vibration of the SiO_2 thin film.

The shifting of Si-O-Si stretching band of silicon dioxide infrared spectra after annealing at different temperatures are given in table 8. As represented in Table 8, the shifting of the Si-O stretching band depends on both

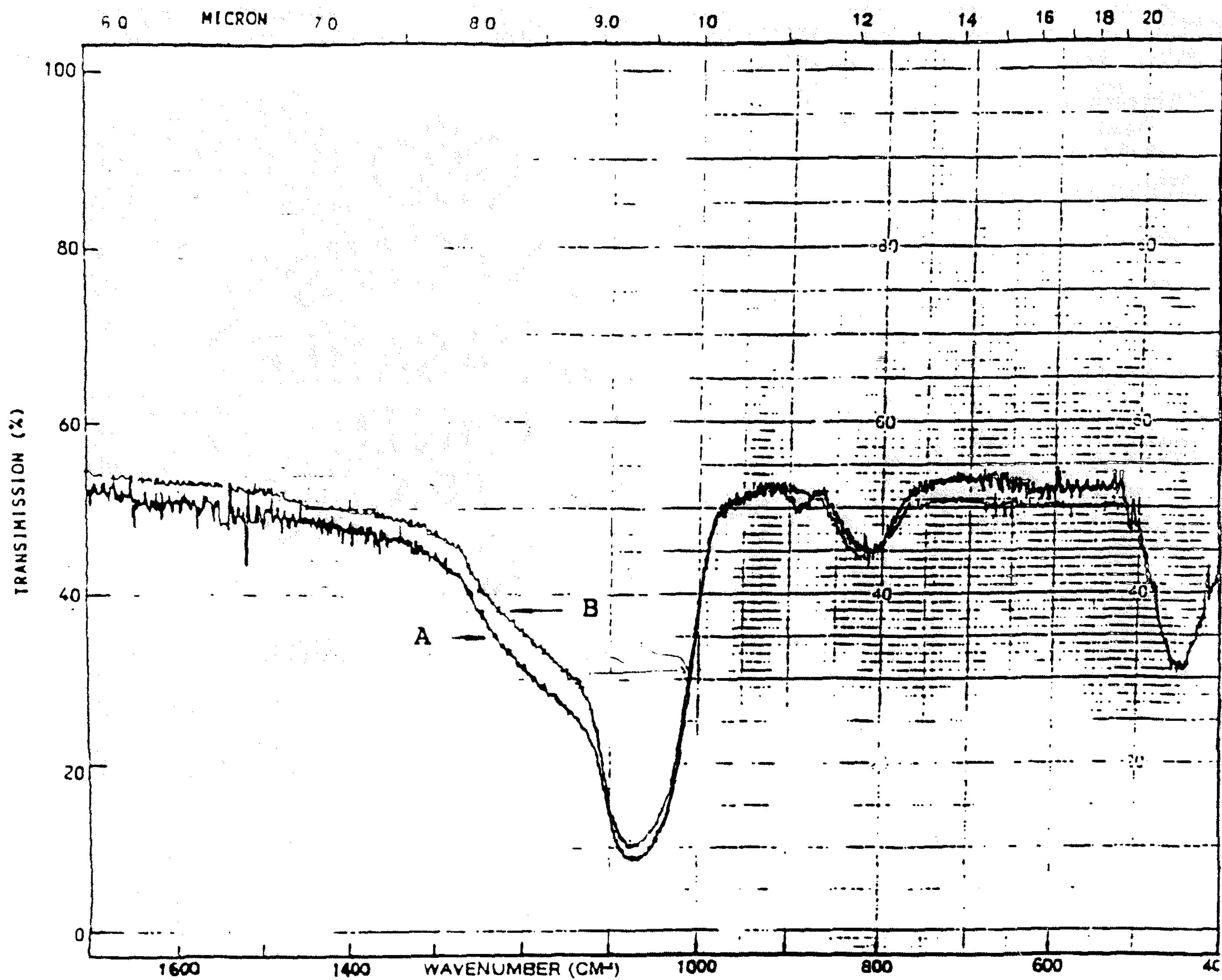

Figure 10. Infrared spectra of SiO_2 at different deposition temperature.
(A), J95, 375 ^{o}C; (B), J101, 475 ^{o}C.

both the temperature of deposition and annealing. The spectra of sample J101 and J95 (annealing at 600°C) is given in Figure 11 and 12 respectively. In Figure 11, spectrum A is that of silicon dioxide film formed at 475°C (J101) and spectrum B is the same film after having been densified in vacuum at 600°C for 1 hr. There is no shifting can be found in Figure 11 after annealing at 600 for sample J101. As expect, the Si-O-Si stretching band of sample J95 (deposited at 375°C) is shifted from 1070 to 1082 cm^{-1} after annealing at the same temperature (Figure 12 and Table 8. for sample J95). After thermal annealing it is found that the infrared spectrum of CVD deposited SiO_2 film shows the stretching band shifting to higher frequency. As previously mentioned, the stretching band position of nondensified silicon dioxide films at lower frequency show porous (less dense) and the atomic arrangement is more irregular than that the same film after a annealing.

Table 8. The annealing effects on infrared spectra of SiO_2 films deposited at different temperatures.

sample ID	deposition temp(°C)	annealing temp(°C)	IR band at ~ 1070cm^{-1} before	after	shift(cm^{-1})
J98	425	900	1070	1080	10
J95	375	600	1070	1082	12
J95	375	750	1070	1080	10
J95	375	900	1070	1085	15
J101	475	600	1070	1070	0
J101	475	750	1070	1080	10
J101	475	900	1070	1085	15

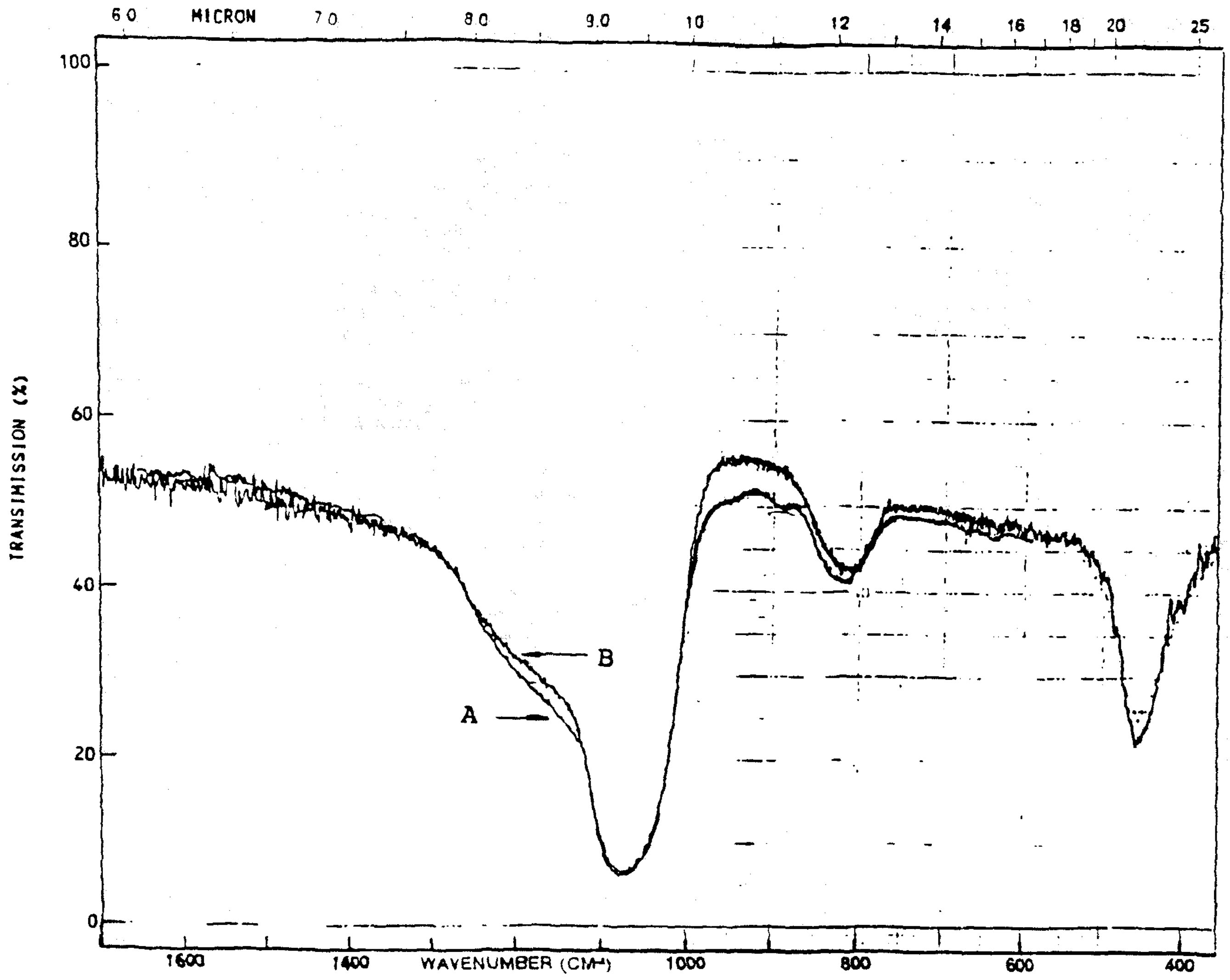

Figure 11. Infrared spectra of SiO_2 film deposited at 475 ^{o}C (J101): (A) initial deposited film; (B) after annealing at 600 ^{o}C 1 hr.

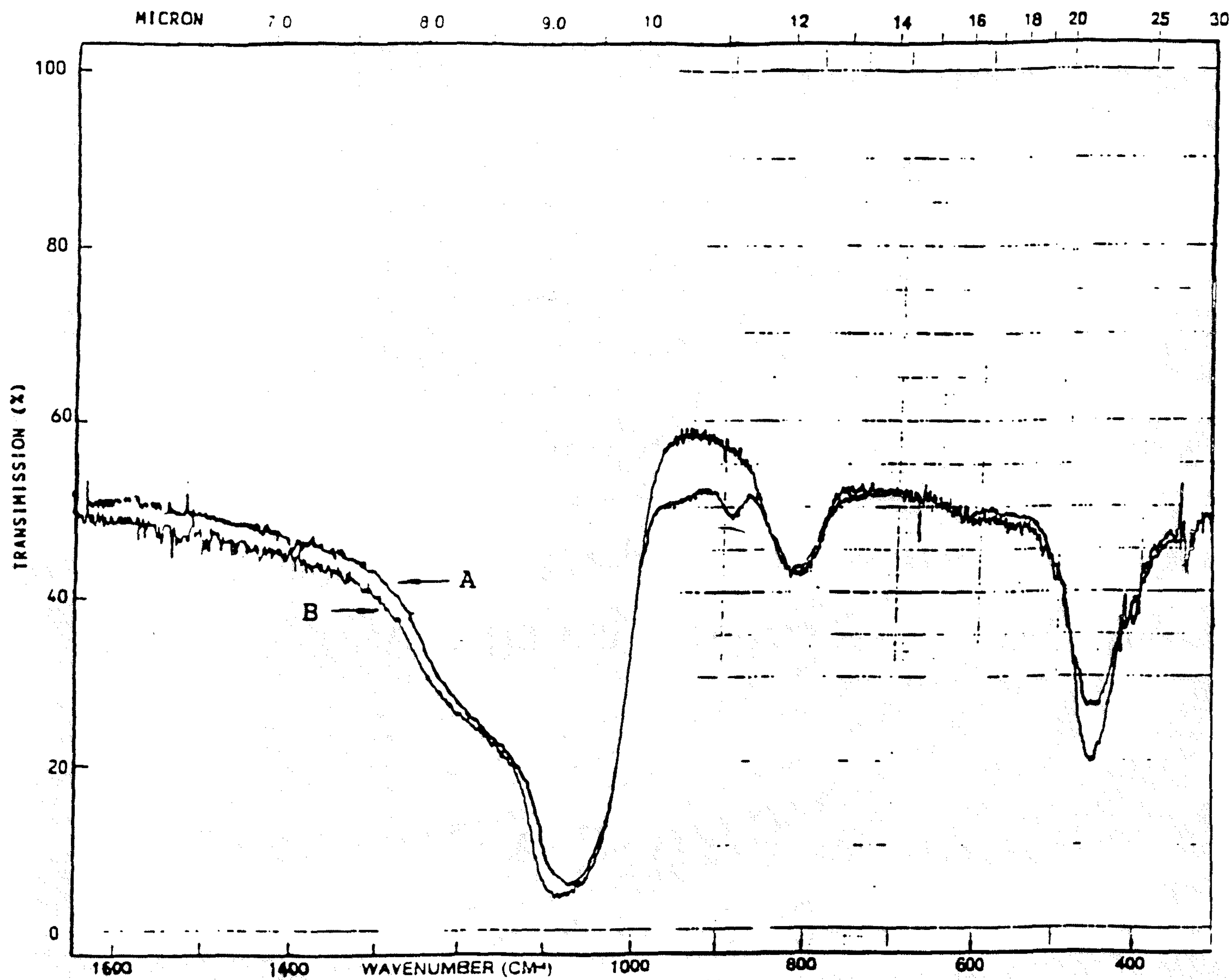

Figure 12. Infrared spectra of SiO_2 film deposited at 375 °C (J95); (A), initial deposited film; (B), after annealing at 600 °C 1 hr.

The degree of shifting is a function of annealing temperature for the same film (Table 8). The stretching band of sample J101 shifted 0, 10, and 15 cm^{-1} to higher frequency at the annealing temperature of 600, 750, and 900°C respectively; and J95 shifted 12, 10, and 15 cm^{-1} over the same annealing temperature range. In Kobeda's the work [17], it shows that the frequency of the bond stretching vibration is approximated by

$$v = v_o \sin \theta \qquad (1)$$

where v is the stretching band frequency at ~ 1070 cm^{-1}, v_o is 1117 cm^{-1} [16], and 2θ is bond angle as indicated in Figure 13. Considering the bonding arrangement in Figure 13 the distance between the Si atoms, d, is related to the Si-O bond length, r_o, by

$$d = 2r_o \sin \theta \qquad (2)$$

Equation (2) shows that the distance between Si atoms in SiO_2 depends directly on the bond angle 2θ at the oxygen atom site, and a shift to lower or higher wave number can be interpreted in terms of a decrease or increase in the Si-O-Si bond angle and the Si-Si distance. The bond angle was estimated to be $147° \pm 10°$ for thermal oxide [15]. The untreated initial deposited SiO_2 films result in related lower frequency and the broader width of the stretching band as a result of large distribution of bond angles. In the other words, the strain of the Si-O-Si molecule causes the band shifting to higher frequency and sharper.

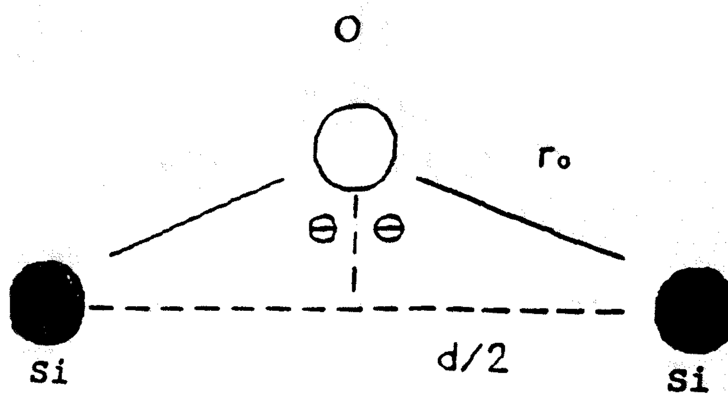

Figure 13. The Si-O-Si bonding arrangement.

ii. The annealing effect on $3u$ band infrared spectra

This section will discuss the results in higher frequency region of infrared spectra of SiO_2. The higher frequency region (~ $3u$) of spectrum where absorptions due to hydrogen bonded SiOH groups (3650 cm^{-1}) and absorbed water (~ 3330 cm^{-1}) occur [28]. It is important because water and silanol groups are the impurity in low-temperature deposited silicon dioxide films. The intensity of these absorptions are an indication of the degree of porosity of the film.

Figure 14, 15 represented a weak absorption in the 3u region of sample J101 and J95 respectively. In spectrum A of Figure 14, sample J101 was deposited at 475°C , and spectrum B is that of the same sample was densified in vacuum at 900°C for 1 hr. By comparison with the spectrum of initial deposited film in Figure 14, it shows that the densification was sufficient to remove the adsorbed water. The similar result of sample J95 which was densified at 600°C is given in Figure 15.

Details on the characterization of silicon dioxide films in this region have been described in some early publishes [15, 18, 24, 28] . The similar results in this work indicated the presence of residual hydrogen in the form of OH and H2O. It resulted disappearing of the 3u band spectra and obtaining more dense of SiO_2 films after annealing.

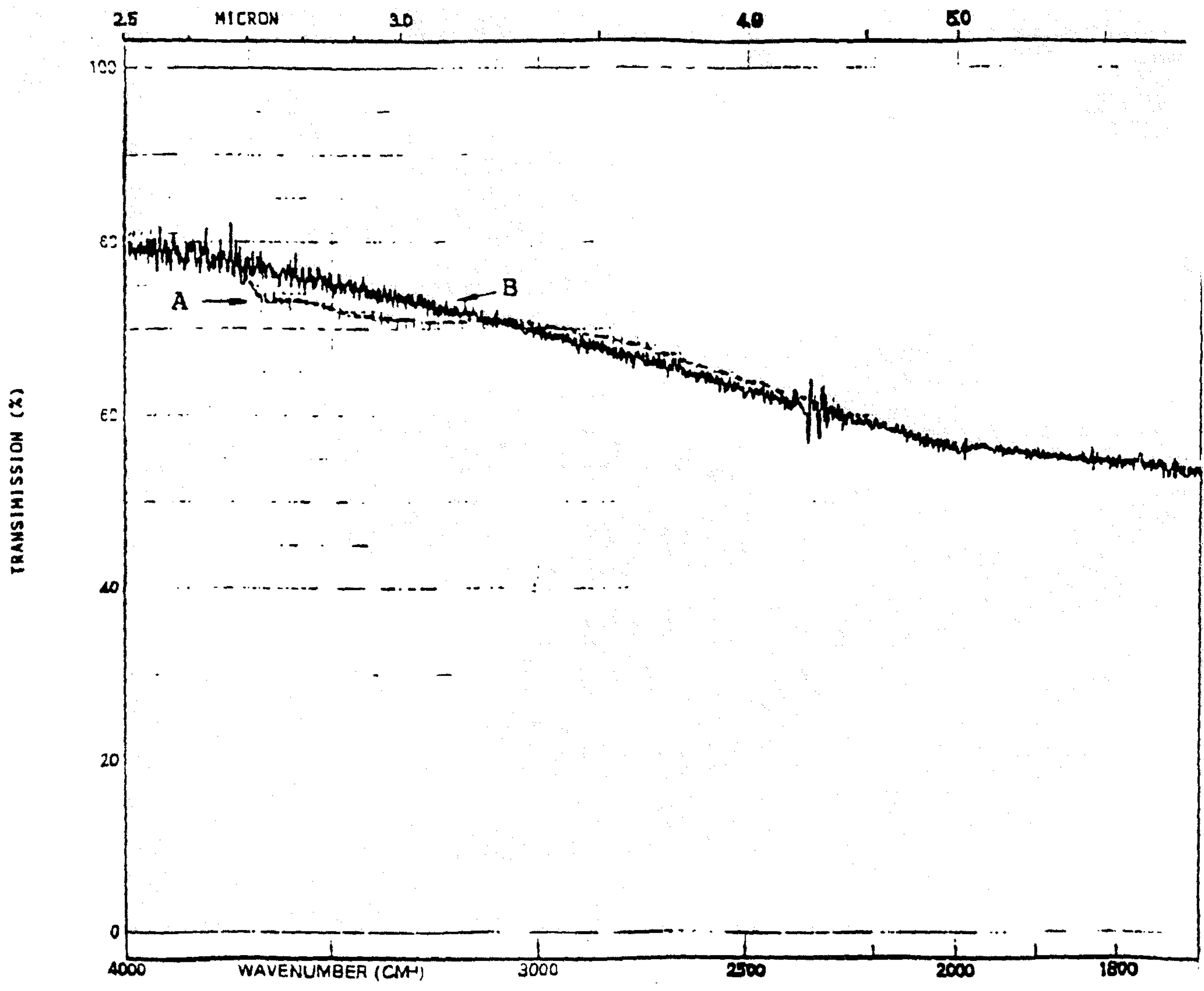

Figure 14 Infrared spectra around 3u band for sample J101 (475°C deposited); (A), initial deposited film; (B), after heating at 900°C 1 hr.

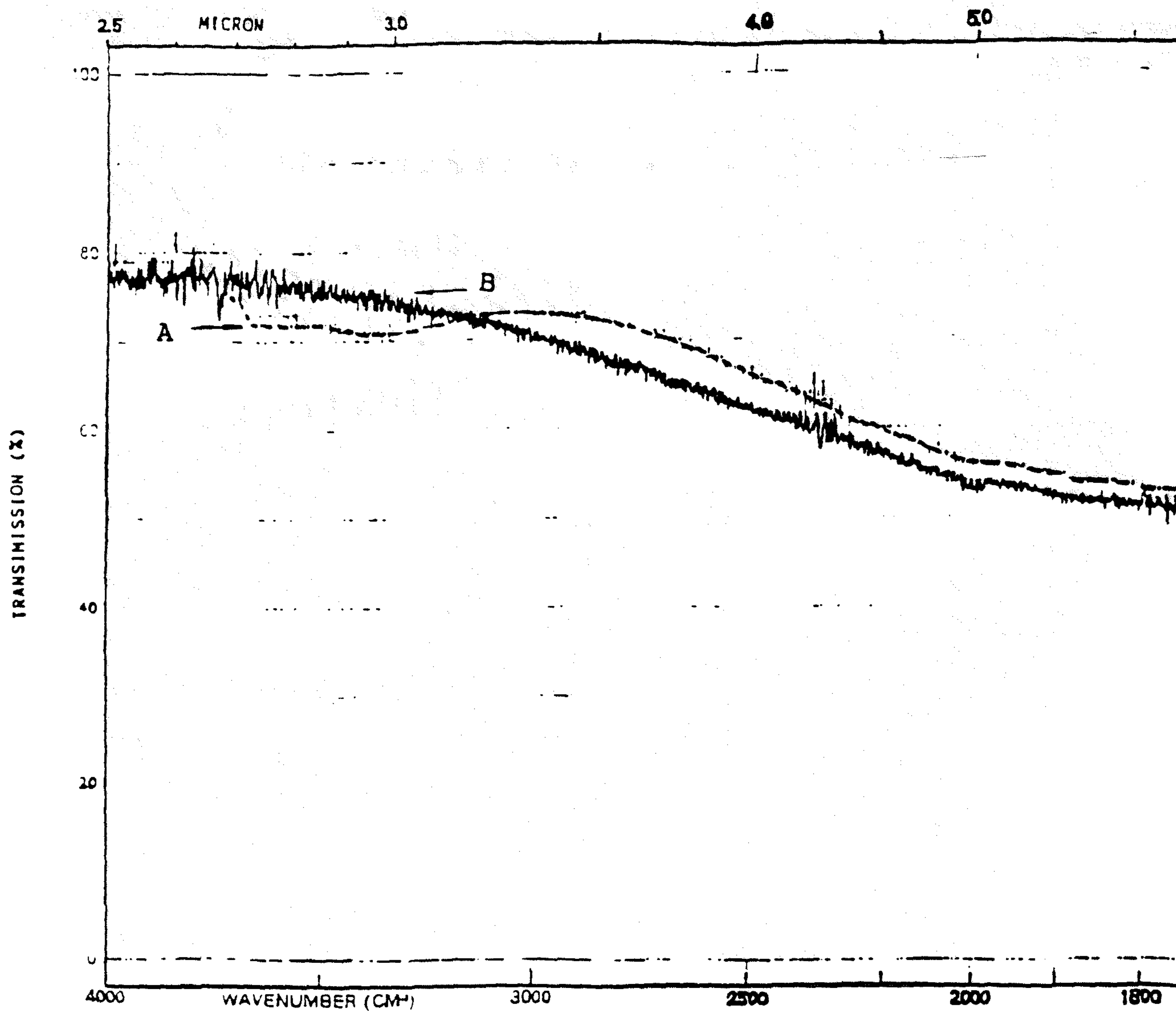

Figure 15. Infrared spectra around 3u band for sample J95 (375 ^{o}C deposited); (A), initial deposited film; (B), after heating at 600 ^{o}C 1 hr .

iii. The annealing effect on a weak band at the frequency of 890 cm^{-1}

From silicon dioxide films deposited at 375 and 475°C, the infrared spectra of these films represented the presence of another very weak band of at ~ 890 cm^{-1} before annealing (Figure 11, 12), and disappear after annealing. Pliskin [18] found a similar band at 935 cm^{-1} from the spectrum of electron-beam-evaporated SiO_2 which was taken after 24 days' exposure to 85% relative humidly at 85°C. He found that this band disappeared after densifying the film by heating for ten minutes at 983°C. Pliskin's result indicated that the 935 cm^{-1} band is attributed to the Si-O-Si stretching vibration strongly hydrogen-bonded silanol (SiOH) groups, thus showing that water has reacted with the SiO_2 to form SiOH (This band can be seen in rest of infrared spectra of our nondensified SiO_2 films). In this work the disappearance of this very weak band after annealing demonstrated that SiOH was removed, due to the more dense structure, the less area for the absorption of the water.

Pliskin *et al'* [33] study shows that the slower deposition rates and for the poor vacuum conditions films of higher oxidation states can be formed including an intermediate type of oxidate that produces a weaker intensity band near 870 cm^{-1}. This is believed to be Si_2O_3, and it has a refractive index intermediate between those for

SiO_2 (1.45) and SiO (1.99) [38]. In order to avoid oxygen deficiency, the oxygen to silane ratio should be greater than 10 [33], as in the case of low-temperature-oxidation of SiH_4. When this ratio falls below four, Valletta *et al.* [34] observed an absorption at about 870 - 880 cm^{-1}, attributed to the oxide inter-mediate Si_2O_3. Generally, when this band is present, there is also an absorption band at 2170 cm^{-1} due to Si-H.

In this work, the presence of the weak band of SiO_2 spectrum at ~ 890cm^{-1}, it can be confirmed by the refractive index measurement before and after the densification with the same value of $n = 1.45$, shows that the film is exactly SiO_2. The absence of the band at about 2170 cm^{-1} substantiates that 890 cm^{-1} band is due to the extra water absorbed by SiO_2.

4.2.4 Effect of DES flow rate on Si-O-Si stretching band

The amount of band shifting in infrared spectra for the DES flow rate series are given in Table 9. The band shifting in infrared spectra after annealing is independent of DES flow rate. This fact demonstrates that the structure of the CVD silicon dioxide films with different flow rates is almost the same. It agrees with the etch rate study (see details in section 4.3.1, page 51).

Table 9. The annealing effects on infrared spectra of SiO_2 films deposited at different DES flow rates.

sample ID	deposition temp(°C)	annealing temp(°C)	IR band at ~ 1070cm-1 before	after	shift(cm-1)
J56		900	1075	1085	10
J47		900	1075	1085	10
J74		600	1070	1085	5
J74		750	1070	1080	10
J74		900	1070	1085	15

4.2.5 Effect of annealing temperature on Si-O-Si stretching band (DES flow rate series)

Table 9 also shows that with the same annealing temperature (900°C), the amount of shifting of the Si-O-Si stretching band does not vary with DES flow rates. This attributed to the same molecular strain of SiO_2 films with different DES flow rates.

4.3 ETCHING RATE

A few samples were immersed in p-etch solution at room temperature for a short term (about 30 sec.), after which the thickness of the films were measured by Nanospectra. The etch rate was obtained from the slope of thickness verses etching time. (for example see Figure 16.)

As the P-etch rate of silicon dioxide films were measured at room temperature, during the period of the experiments (from July to September) the room temperature was changed in a range of 21° to 26°C. The influence of this change on etch rate were examined and corrected (see section 4.3.4, page 60).

4.3.1 Etching rate of silicon dioxide films with varies DES flow rate

The etching rates of the DES flow rate series SiO_2 samples (see Table 2 for the details) were obtained from the slope of the thickness vs etching time (Figure 16 and Table 10).

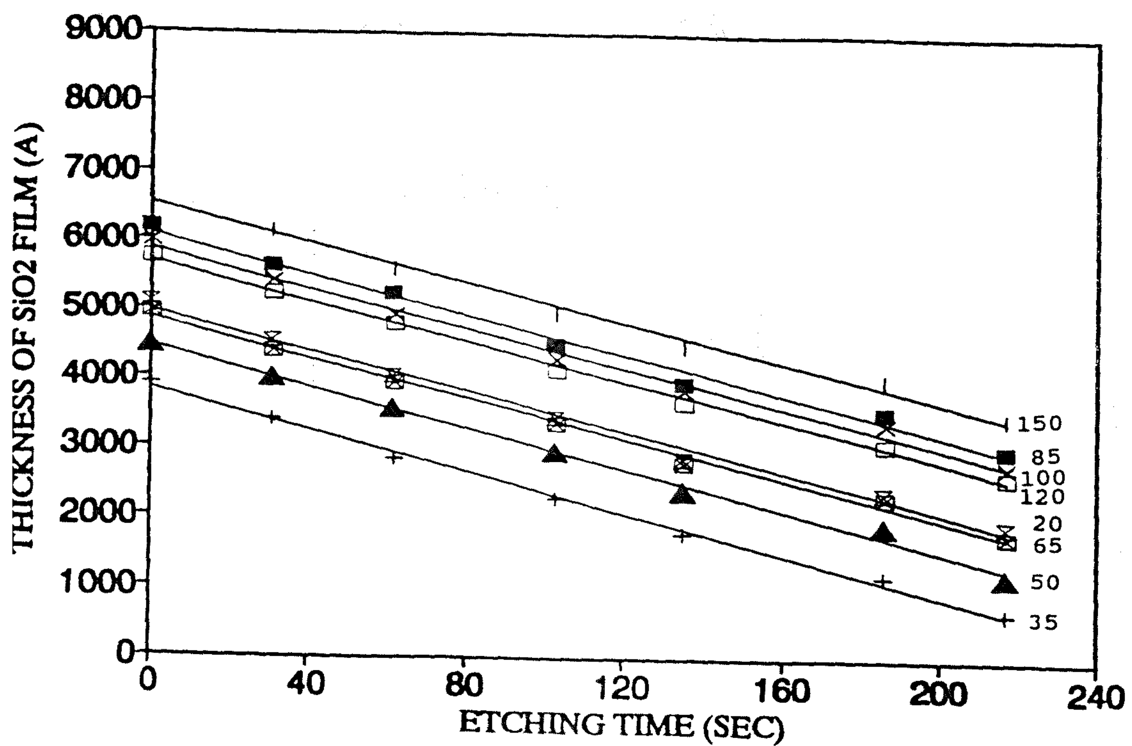

Figure 16. The SiO_2 film thickness vs P-etch time for the DES flow rate series samples. The number following the curves indicate flow rate in sccm.

Table 10. Calculation data of etch rate for DES flow rate series SiO_2 films.

sample ID	J74	J65*	J44	J60	J47	J52	J40*	J56
Flow rate of DES (sccm)	160	120	100	85	65	50	35	20
P-etch rate (A/min)	900	900	900	900	900	920	920	900

* Double side deposition

** See section 4.3.4 for etch rate correction

For the DES flow rate series the etch rates have no significant difference with DES flow rates changing (see Figure 17, page 54).

The similar etching rate around 900A/min for all of the samples were obtained. It agreed with the results in the infrared spectra of this series.

4.3.2 Behavior of etching rate on deposition temperature series

The etch rate of the temperature series were obtained from the slope of the thickness vs etching time are given in Figure 18 and Table 11. As shown in Figure 19, the etch rate of the temperature series varied linear with the deposited temperature. A comparison of the etch rates for the DES flow rate series, and the etch rates for the temperature series indicates that etch rate has a greater dependence on deposition temperature than the DES flow rate.

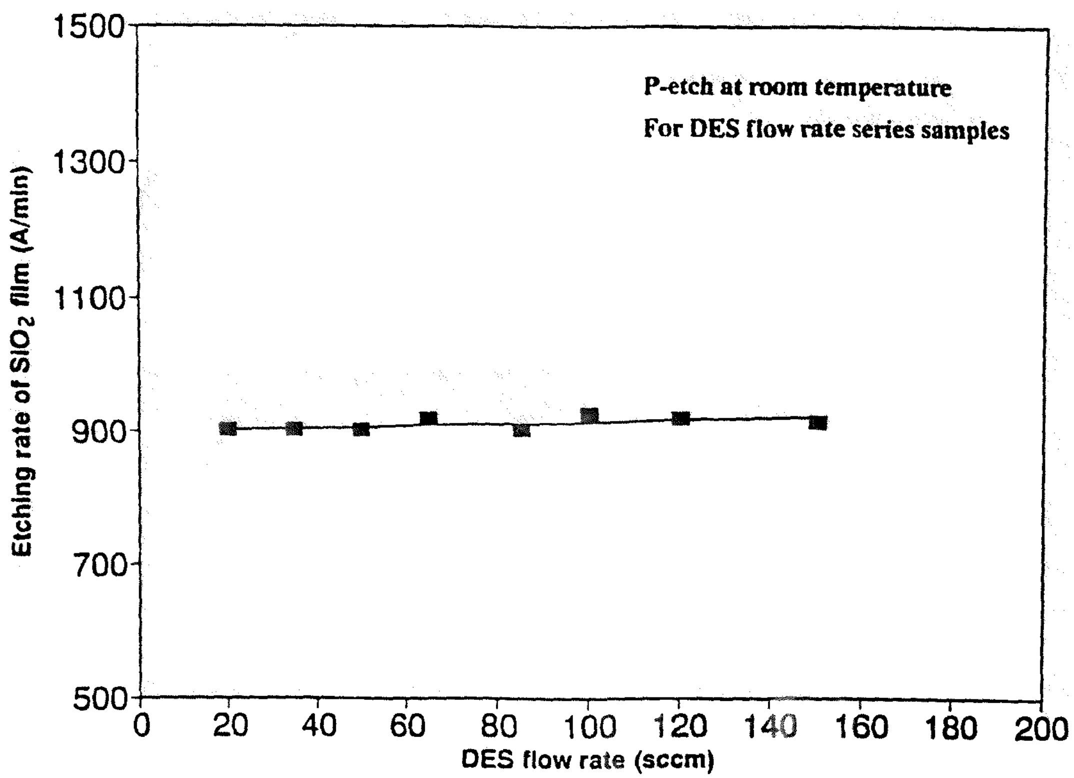

Figure 17. P-etch rate of silicon dioxide film is plotted with DES flow rates.

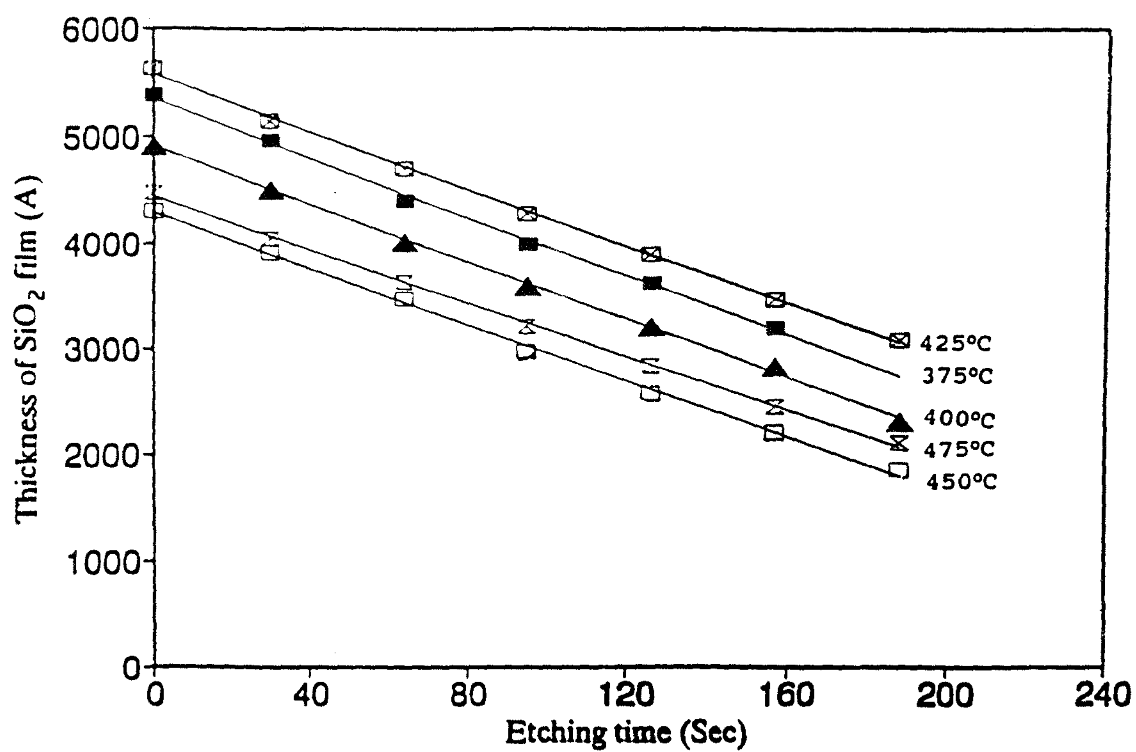

Figure 18. The SiO_2 film thickness vs P-etch time for the temperature series samples.

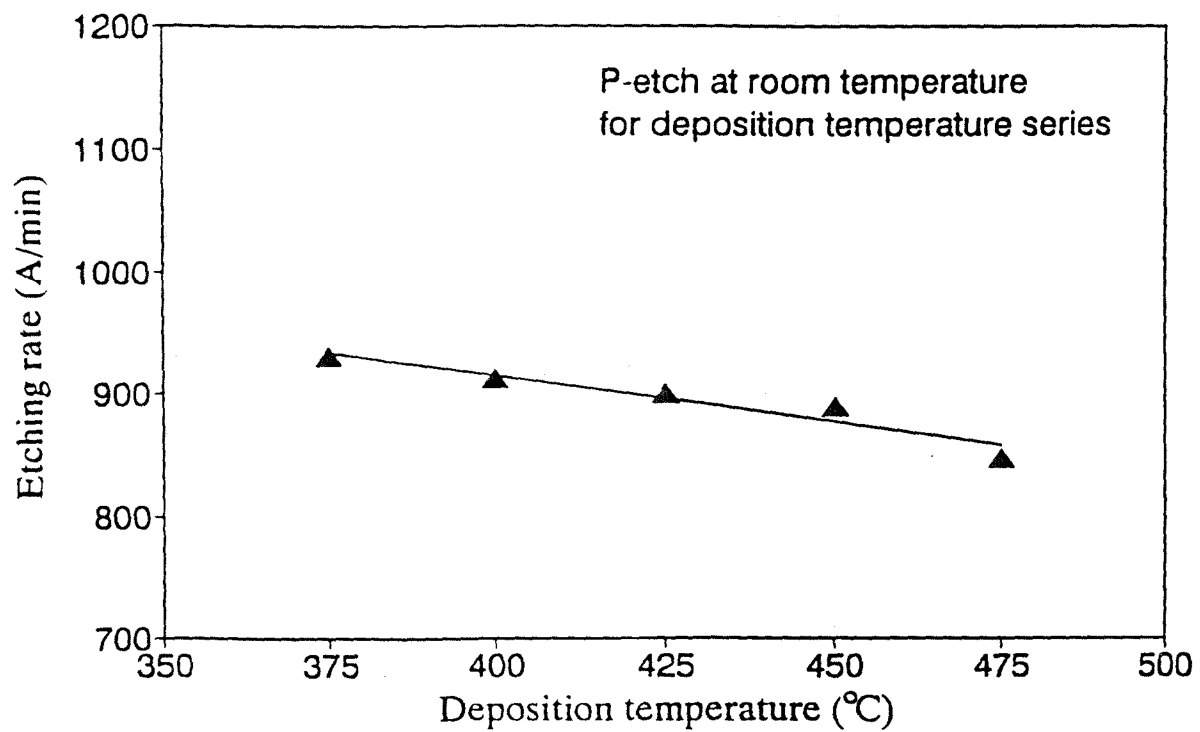

Figure 19. P-etch rate of SiO_2 film is plotted as a function of deposition temperatures.

Table 11. Etch rate of SiO_2 films produced at various temperatures.

sample ID	J95	J92	J98	J104	J101
Deposited temperature (°C)	375	400	425	450	575
P-etch rate (A/min)	930	910	900	890	850

* All of sample of temperature series are double sides deposition.

** See detailed information at section 4.3.4 for etch rate correction.

4.3.3 The different annealing temperature effect on etching rate of silicon dioxide films

The selected SiO_2 film samples underwent the thermal annealing at 600°, 750° and 900°C to vacuum for 1 hour respectively. The etch rate measurement of SiO_2 film shows quite different for all of these samples before and after densification (for example see Figure 20 for sample J95 and Table 12 for all samples). After annealing at 900°C, the P-etch rate of silicon dioxide is about 1/3 of the original value. This result is in agreement with the results obtained from infrared spectra.

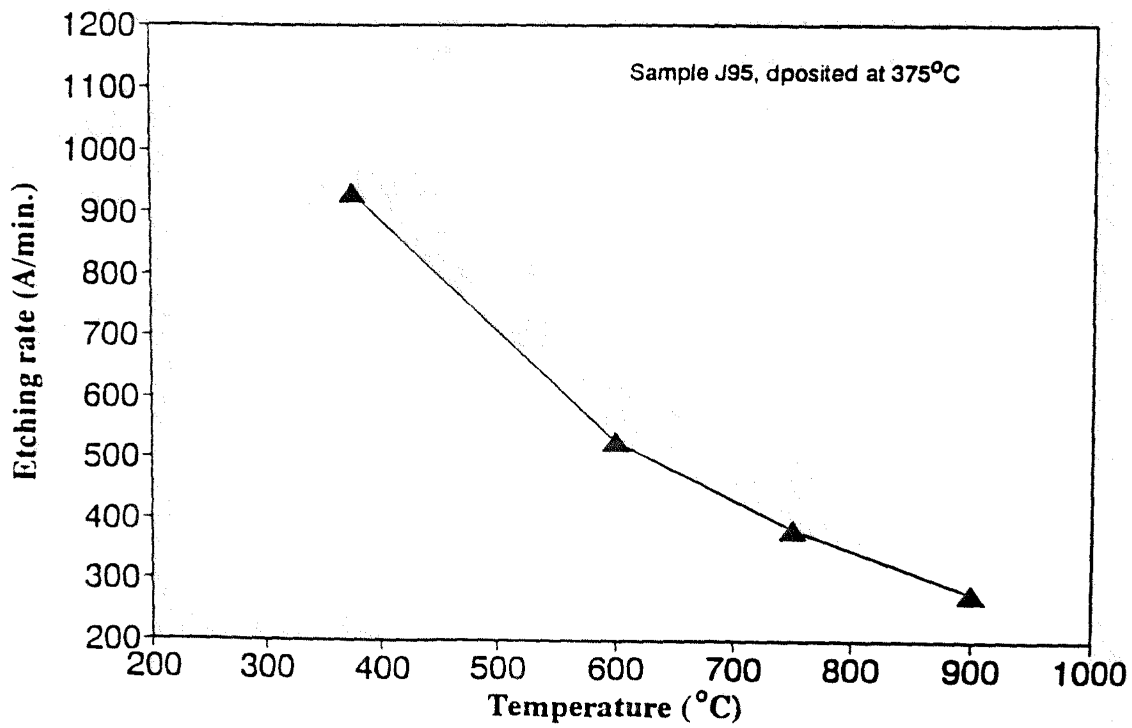

Figure 20. Effect of different annealing temperatures on etch rate of SiO_2 film (J95).

Table 12. Effect of annealing temperatures on etch rate of SiO_2 films (25°C)

sample ID #	etch rate (Å/min.)			
	original	annealing at 600°C	annealing at 750°C	annealing at 900°C
J95	930	530	380	280
J98	900	500	360	290
J101	850	550	340	290
J56	910	590	380	310
J47	900	520	350	300
J74	900	560	360	310

4.3.4 Temperature effect on etching rate of Silicon dioxide films

Temperature has an important influence on the etch rate of silicon dioxide films. The etch studies were performed at room temperature between 23° - 26°C. The influence of temperature on etch rate was examined under various well controlled temperatures at 30, 35, and 40 $\pm$ 0.02°C in a water bath. A plastic container (with a cover in order to avoid the vaporizing) with etchant was put in the bath. The experiments were started at room temperature (~25°C), heated for 5 minutes for each additional 5°C and left for 35 minutes to achieve temperature equilibration.

Three samples with different deposition conditions (see

detailed in Table 2 and 3) were examined at different temperature. At the same examined temperature the similar etch rates of were obtained for those samples (Table 13).

The etch rate varying with temperature changing were obtained from the slope of the etch rate of silicon dioxide verse different temperatures (Figure 21). The average value of etch rate of silicon dioxide changing with the temperature varying per degree (Celsius) is 0.8 A/sec. The etch rates obtaining at different temperature were corrected by this factor to room temperature 25°C as shown in Table 10, 11, 12.

Table 13. Temperature effect of etch rate of silicon dioxide.

sample ID #	etch rate (A/sec)		
	30 °C	35 °C	40 °C
J92	15.83	21.26	26.22
J44	16.03	18.79	22.06
J60	15.65	19.69	23.41

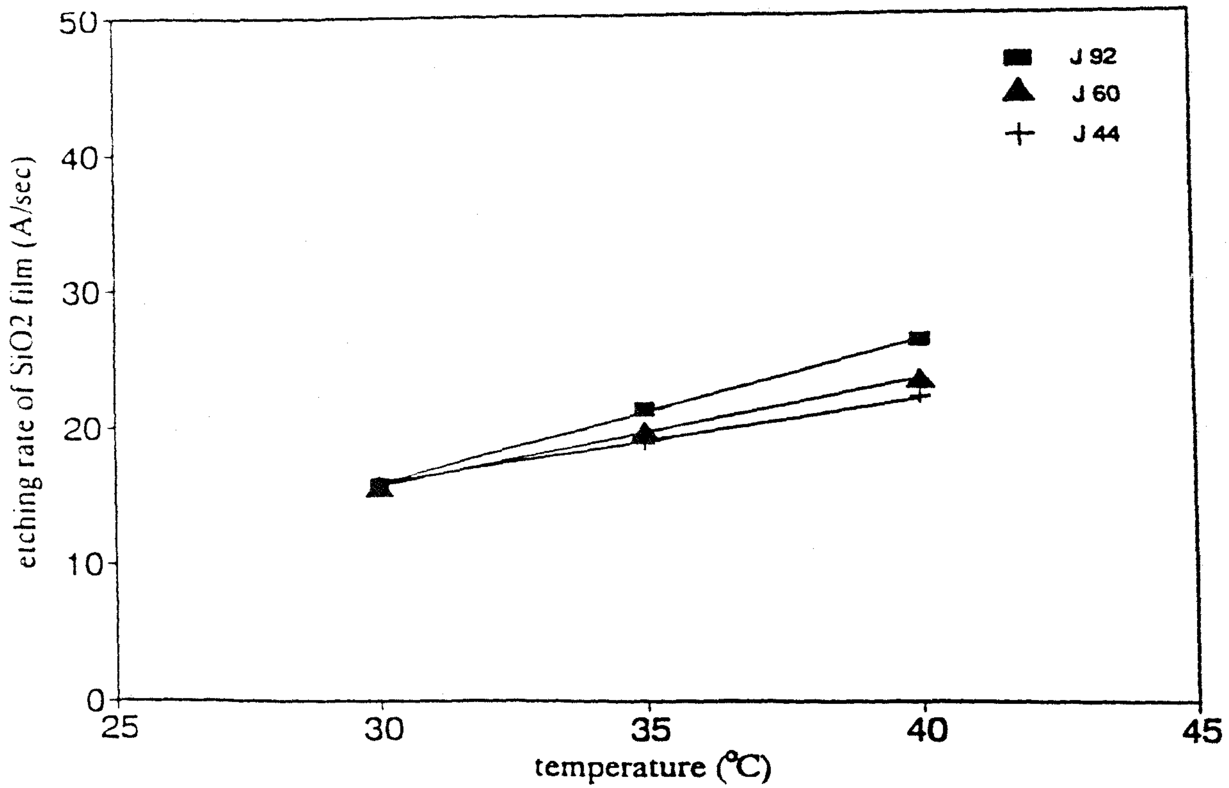

Figure 21.P-etch rate of silicon dioxide as a function of measured temperature.

4.4 REFRACTIVE INDEX MEASUREMENT

4.4.1 Refractive indices of deposition temperature series silicon dioxide films

The result of the refractive index measurements of the temperature series SiO_2 film samples is given in Figure 22. The refractive index was constant for all samples of this series. The refractive index has the same consistence for the samples in the DES flow rate series.

4.4.2 Effect of wafer's position on refractive index measurement and thickness

In the horizontal low-pressure reactor, the gases are inserted from one end of the reaction chamber, and flow along the wafer loading. For efficient utilization of the silicon containing gas, its partial pressure must decrease along the wafer loading. Unless compensated, this gas depletion causes the deposition rate to decrease along the wafer load, with variations in film thickness. The uniformity of the film at the different load position were examined by measuring the thickness, refractive index and calculated SiO_2 density. The samples were selected in the run #25. The temperature was 450°C, the DES flow rate was 150 sccm with the ratio of O_2/DES was 2, and the pressure

was 0.5 Torr. The manner of wafers location in the chamber is given in Table 14, it also shows the thickness, refractive index, and the density of these SiO_2 films. The thickness were measured in different manner, 5 points and 4 points, with average infractive index of 1.45 respectively. The density were calculated with these different manner.The details is discussed in the following section.

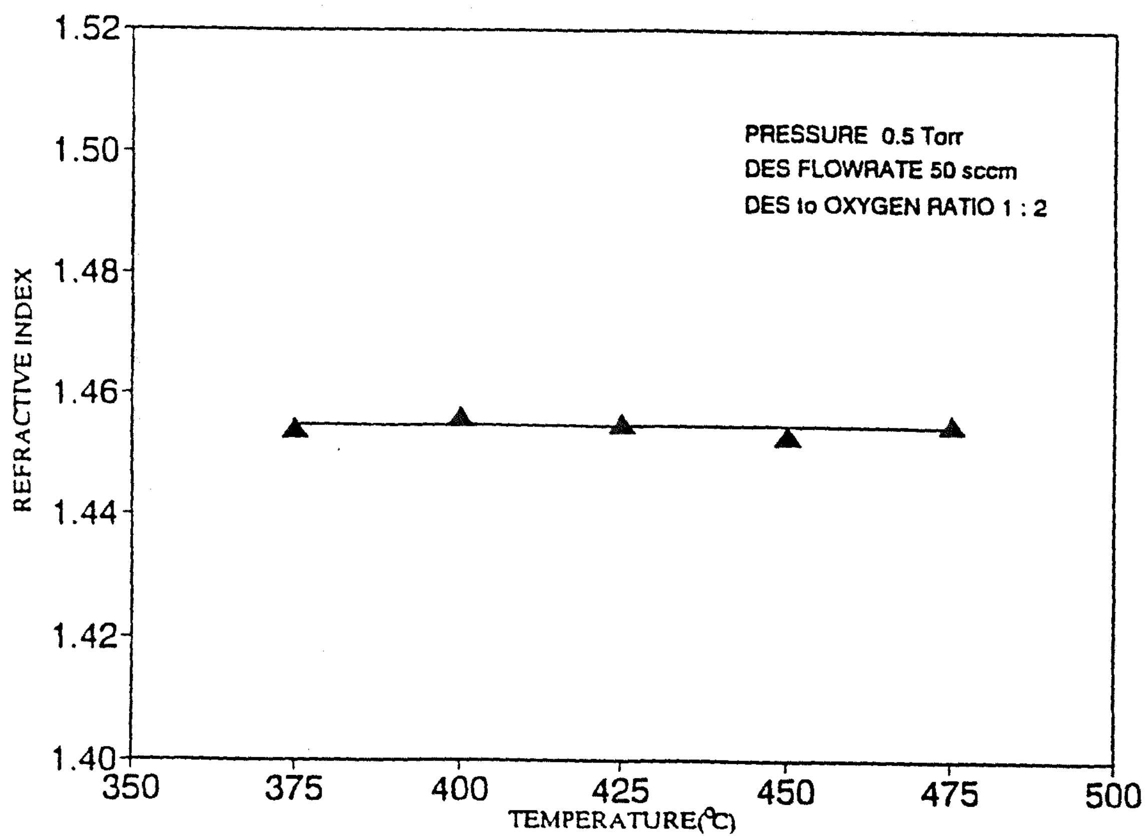

Figure 22. Refractive index of silicon dioxide as a function of deposition temperatures.

Table 14. The refractive index, thickness, and calculated density of the SiO_2 film from run #25.

Position of wafers loaded in the chamber

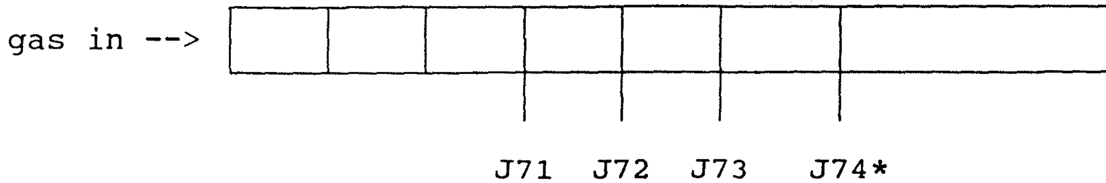

sample	J71	J72	J73	J74	mean	
center index	1.452	1.455	1.447	1.444	1.45	
mass deposi.	28.4	26.8	25.4	15.1	-----	(mg)
T(5 points)A	8499	8108	7865	7244	-----	
dens.(g/cm^3)	2.10	2.07	2.02	2.64	2.01	2.05±0.04(A1)
T(4 points)A	8352	7976	7752	-----	7786	
dens.(g/cm^3)	2.16	2.13	2.08	-----	2.07	2.11±0.04(A2)
dens.(g/cm^3)	2.28	2.25	2.20	-----	2.19	2.23+0.04(A3)

* single side deposition
A1 Average density calculated from 5 points measurement.
A2 Average density calculated from 4 points measurement.
A3 Density calculated with the thickness ratio of front/back side = 1.12 from Run #50 wafer # J139, from 4 points measurement.

4.4.3 density of CVD deposited SiO2 film (uniformity of film)

In Table 16 it can be seen that the wafer position in the chamber effects a changing of the film properties, such as thickness, refractive index, and the density. This effect comes from the concentration gradient of the reactant gas in the tubular. The thickness is decreasing as the wafer position increasing from the gas inlet, in the decreasing concentration direction. The refractive index changed in the same direction. Deposition using a double sides polished wafer yield a front (T_f) and back side (T_b) thickness which vary little, the ratio of T_f/T_b is 1.12. (wafer J139). This ratio indicates the presence of a somewhat difference of the reactant gas concentraion in front and back side of the wafer. The face to the gas inlet direction has a slightly higher concentraion than the back side. The value of density obtained after the thickness correction with this ratio is 2.23 g/cm^3, the same as in early work [18].

The uniformity of the film across the whole wafer was examined. The thickness measured upon the whole wafer in the different direction is given in Figure 23 and 24 for the horizontal and the vertical direction respectively. It can be seen clearly from these two graphs, that the thickness changed quite much in either horizontal or vertical direction. It is going thicker from the center to the edge of the wafer.

Usually, the diameter of the chamber is slightly large than that the size of the wafer and the loading boat together. This desired size of the reactor and the loading wafer resulting good uniformity of the film. But in this experiment as previously mentioned in chapter 3, section 3.1 (Page 12), the inner diameter of the reactor is 19.1 cm, but the total size of the wafer and the boat together is 11 cm in one direction. As the wafer and boat were put at the bottom of the reactor, the more space above and aside the loaded boat and wafer affects the flow pattern of the reactant gas. So that the ununiformity film formed.

In this study the thickness were obtained from the average of 5 points measurement (as indicated in Figure 24). As can be seen from the profile of the whole wafer's thickness, the 5 point thickness measurement has 3 points on the "thicker" edge. If the average value of two horizontal points (point 3 and 4 in Figure 24) is used instead of two points, the end result by using the mean value of 4 points instead of 5 points, can obtain the value of the thickness (Table 14). The better statistic weight resulted the calculated density of CVD deposited silicon dioxide close to the literature value of 2.2 g/cm3 [18]. The influence of the calculation of density can be found in Table 14.

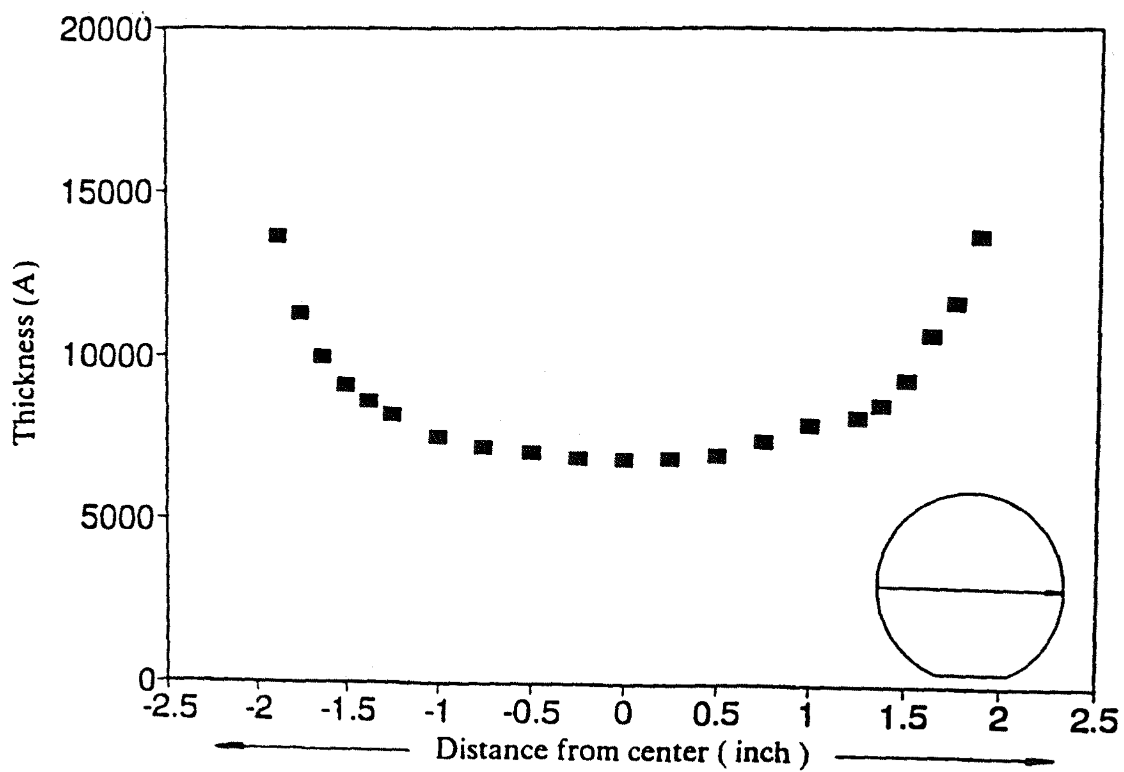

Figure 23. Thickness profile of SiO_2 film (in horizontal direction).

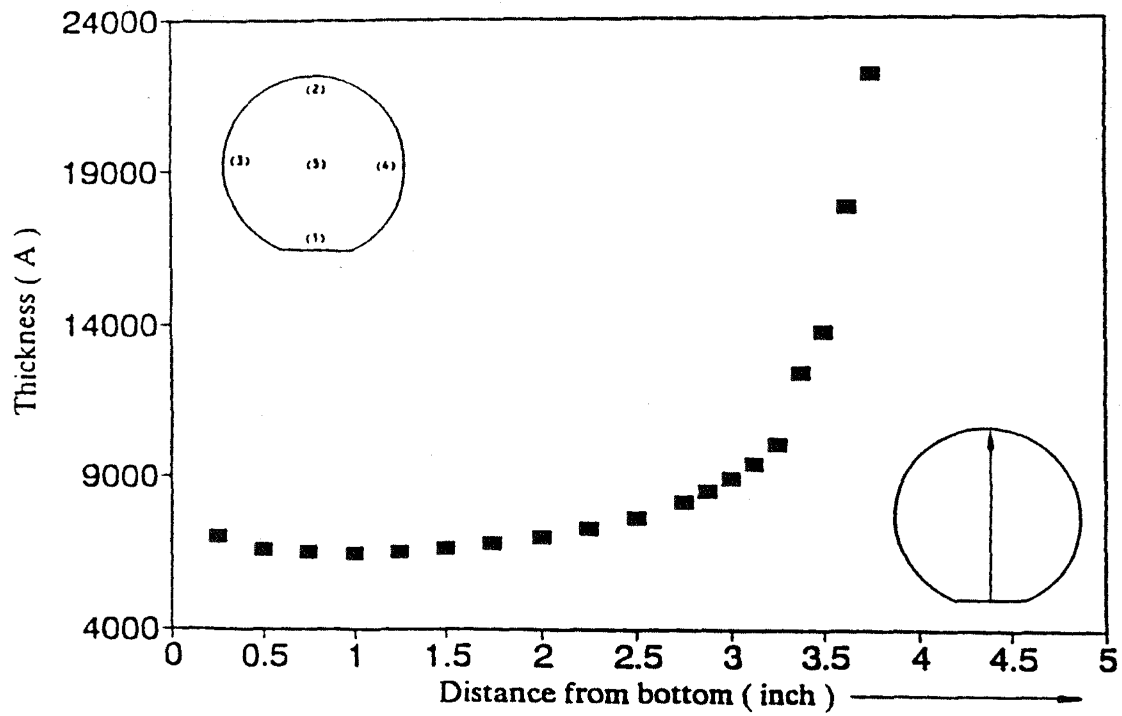

Figure 24. Thickness profile of SiO_2 film (in vertical direction).

5. CONCLUSION

On the basis of the described results, the following conclusions can be made:

I. Silicon dioxide films can be characterized on the basis of refractive index, etch rate, infrared spectra, and thermal densification.

II. Films formed by low temperature have generally inferior properties to those formed by high temperature. However, deposition temperature has more influence than others.

III. Porous and strained oxides can be densified to be indistinguishable from thermal oxides.

IV. Surface of silicon dioxide reacted SiOH can be removed by densification.

V. For a proper evaluation and differentiation of similar silicon oxide films, all of the described techniques must be accurately utilized.

Bibliography

[1]. A.Sherman
Chemical Vapor Deposition for Microelectronics
Noys Publications, New Jersey (1987).

[2]. William C.O'Mara, Robert B.Herring, and P.Hunt
Handbook of Semiconductor Silicon Technology, Noys Publication, 1990.

[3]. R.C.Sangster, E.F.Maverick and M.L.Croutch
"Growth of silicon crystals by a vapor phase pyrolitic deposition method"
J.Electrochem.Soc., v.104 (1957) 317-19.

[4]. H.Schroeder
"Oxide layers deposited from organic solutions" IV
Physics of thin film , v.5 (1969) 115.

[5]. N.Goldsmith and W.Kern
"The deposition of vireos silicon dioxide films from silane"
RCA Rev., v.28, (1967) 153.

[6]
"Comprehensive Inorganic Chemistry" EDITORIAL BOARD
J.C.Bailar, JR.,Urbana
H.J.Emeleus, F.R.S.Cambridge
SIR Roland Nyholm, F.R.S., London
A.F.Trotman-Dickenson, Cardiff
Editorial Board
Pergamon Press (1973) 1388.

[7]. J.Klerer
"On the mechanism of the deposition of silica by pyrolytic decomposition of silanes"
J.Electrochem.Soc., v.112, No. 5 (1965) 503-06.

[8]. J.Klerer
"A method for the deposition of SiO2 at low temperatures"
J.Electrochem.Soc., v.108, No.11 (1961) 1070.

[9]. A.K.Hochberg, A.lagendijk and D.L.O'Meara
"Silicon oxide deposition from cyclic siloxane precursors"
Abstract No.239 P.335.

[10]. A.K.Hochberg, and D.L.O'Meara
"The LPCVD of silicon oxide films below 400oC from liquid sources"
J.Electrochem.Soc., v.136, No.6 (1989) 1843.

[11]. C.S.Gorthy
"Low temperature synthesis and characterization of silicon dioxide dielectric films using diethylsilane"
unpublished paper, Dec.1991.

[12]. W.A.Pliskin, and R.P.Gnall
"Evidence for oxidation growth at the oxide-silicon interface from controlled etch studies"
J.Electrochem.Soc., v 111 (1964) 872.

[13]. W.A.Pliskin and E.E.Conrad
"Nondestructive determination of thickness and refractive index of transparent films"
IBM J.Reasearch & Dev., v.8 (1964) 43.

[14]. D.A.Skong
Principle of Instrumental Analysis, 3rd Ed.
Saunders College Publishing, 1985.

[15]. Joe Wong
"A review of infrared spectroscopic studies of vapor-deposited dielectric glass films on silicon"
J.Electron.Mater., v.5, No.2, (1976) 113-60.

[16]. W.A.Pliskin
in Semiconductor Silicon edited by H.R.Huff and R.R.Burgess
Electrochemical Society, Princeton, NJ (1973) 506.

[17]. E.Kobeda, M.Kellam, and C.M.Psburn
"Rapid thermal annealing of low-temperature chemical vapor deposited oxides"
J.Electrochem.Soc., v.138, No.6 June (1991) 1846-49.

[18]. W.A.Pliskin
"Comparative evaluation of thin glass films"
"Measurement techniques for thin films"
Edited by Bertram Schwartz and Newton Schwartz,
Electrochem.Soc. New York, (1967) 280.

[19]. Scotten W.Jones and Steven T.Walsh
"Wet Etching for semiconductor fabrication"
Jan, 1984.

[20]. W.Kern
"Chemical etching of dielectrics " in "Etching for pattern Definition"
Eletrochemical Society (1976).

[21]. W.Kern
"Analysis of glass passivation layers on integrated-Circuit pellets by precision etching"
RCA rev., 37 March (1976) 78-106.

[22]. J.S.Judge
"A Study of the dissolution of SiO2 in acidic fluoric solution"
J.Electrochem.Soc., v.118(11) (1971) 1772-5.

[23]. W.A.Pliskin
"The evaluation of thin film insulators"
Thin Solid Films, v.2 (1968) 1-26.

[24]. Brown, D.M., W.E.Enqeler, M.Garfinkel, and F.K.Hewmann
"A new masking technique for semiconductor processing"
J.Electrochem.Soc., v114 (1967) 730.

[25]. I.Haller, M.Hatzakis, and R.Srinivasan
"High-resolution positive resists for electron-beam exposure"
IBM J.Res.Dev., v.12 May (1968) 251.

[26]. J.LAWRENE
"Controlled etching of silicon dioxide in buffered hydrofluoric acid"
Proc.Symp.Oxide-electrolyte Interfaces, 1972 (Published 1973) 171-180.

[27]. L.I.Maissel & R.Glang
Hand book of thin film technology
McGRAW-HILL BOOK COMPANY (1970).

[28]. W.A.Pliskin, and H.S.Lehman
"Structural evaluation of silicon oxide films"
J.Electrochem.Soc., v 112 (1965) 1013.

[29]. Karl Riedling
Ellipsometry for Industrial Applications
Springer-Verlag/Wien New York (1988).

[30]. D.J.Gillespie
"A survey of thin film thickness measurement methods"
Measurement techniques for thin films
Edited by Bertram Schwartz and Newton Schwartz, Electrochem.Soc. New York, (1967) 109.

[31]. K.H.Behrnt
"Film-thickness and deposition rate monitoring devices and techniques for producing films of uniform thickness"
Physics of Thin Films, v.3 (1966) 1.

[32]. W.A..Pliskin
"Comparison of properties of dielectric films deposited by various methods"
J.Vac.Sci.Technol., v14, No.5 Sept/Oct. (1977) 1064-71.

[33]. W.A.Pliskin, D.R.Kerr, and J.A.Perri
"Thin glass films"
Physics of Thin Films, v.4 (1967) 257-324.

[34]. R.M.Valleta, W.A.Pliskin, D.W.Boss, and V.Y.Doo,
The Electrochemical Society meeting at New York, May (1969);
Ext.Abs No.43.